

# Physics with photons in ATLAS



L. Carminati  
(Universita' e sezione INFN di Milano)  
On behalf of the ATLAS collaboration



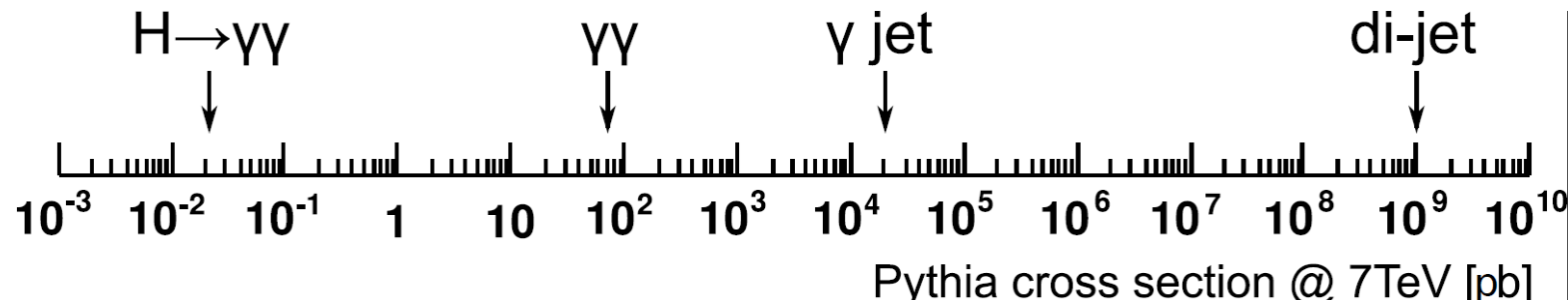
---

## What with photons in early and 'not so early' data?

- ❑ Measurement of the single / double photon production cross sections (+ all the relevant distributions ), photon+jet,  $Wg/Zg$  ([arXiv:1106.1592v1](#))
  - ❑ test of QCD predictions.
  - ❑ Use direct photons as an input for PDFs: direct photons can be used to probe the gluon content of the proton. Check the predictions in eta distributions (for example) varying the PDFs sets. Hopefully direct photon data could play a role in the PDF fits again
  - ❑ probe our capability to perform convincing measurements involving photons
  - ❑ main backgrounds for many 'discovery' channels
- ❑ Can we say something at least on the presence of new physics?
  - ❑ Search for Higgs decays into two photons ([ATLAS-CONF-2011-085](#))
  - ❑ Observe or exclude gravitons decaying into a 2 photons pair ([ATLAS-CONF-2011-044](#))
  - ❑ Some SUSY and Universal Extra Dimensions models predict new physics with photons ([Phys.Rev.Lett.106:121803,2011](#) )

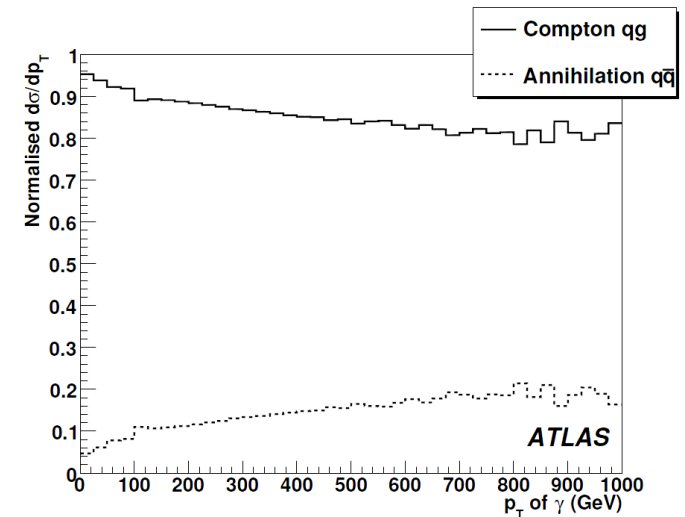
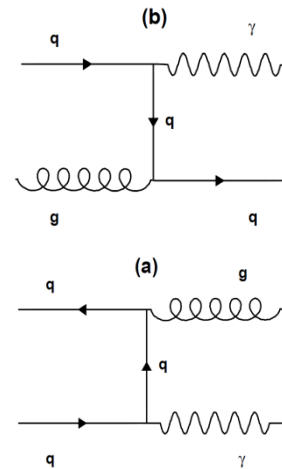
## The challenges in photon physics :

- ❑ QCD dijet production cross section is order of magnitudes larger than the signal : excellent jet rejection ( $\sim 10^3$ - $10^4$ ) capability of the detector is required to extract the signal over the background
- ❑ In general don't want to trust too much on the MC information and try (as much as possible) data driven techniques to estimate the photon yields
- ❑ No clean source of photons (no decays like  $Z \rightarrow e e$  unfortunately) to be used to check photon efficiency and calibration using some tag and probe technique.

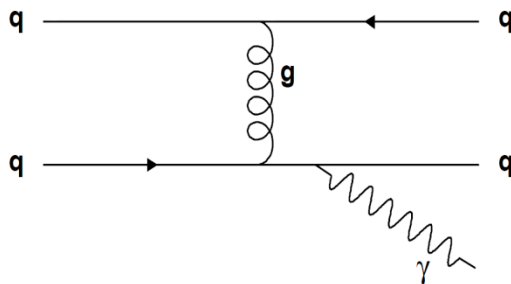


## The prompt photon production and the 'fragmentation' issue :

- ❑ Direct : at LO the contribution to direct prompt photon production is (relatively) easy. It is given by the processes in the plots : all these are order  $O(\alpha\alpha_S)$  .
- ❑ Fragmentation (a photon behaves like an anomalous hadron coming from the collinear fragmentation of a coloured high  $p_T$  parton)

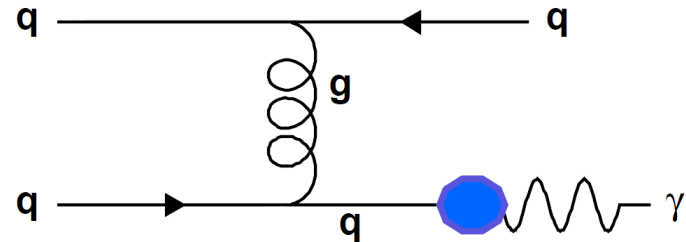
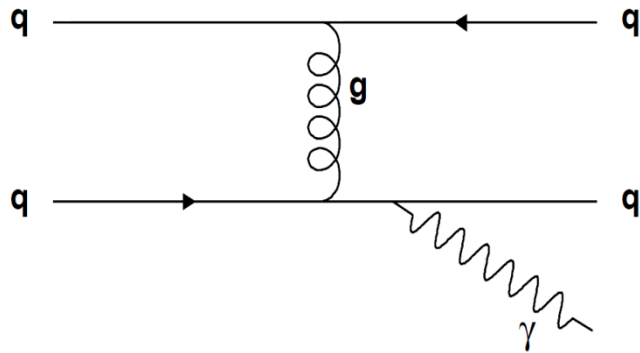


- ❑ Technically the fragmentation contribution emerges from the HO corrections to Born process: at NLO collinear singularities occur in the calculation of the contribution for example from the subprocess  $qq \rightarrow qq\gamma$



These singularities are factorized and absorbed into  $q/g$  fragmentation functions into photons  $D_{q\gamma}(M_F)$  and  $D_{g\gamma}(M_F)$  : these functions can't be calculated and are determined experimentally (see for example LEP measurements, hep-ex/9708020v1, CERN-PH-EP-2009-014)

## The 'fragmentation' within a full NLO calculation



$$d\sigma(AB \rightarrow \gamma X) = \sum_{a,b,c,d} \int dx_a \int dx_b F_{a/A}(x_a, M) F_{b/B}(x_b, M) \times [d\sigma^{dir} + d\sigma^{frag}]$$

$$d\sigma^{dir} = d\sigma^{ab \rightarrow cd}(x_a, x_b, \mu, M, M_F)$$

$$d\sigma^{frag} = \int \frac{dz}{z} D_{c/\gamma}(z, M_F) d\sigma^{ab \rightarrow cd}(x_a, x_b, \mu, M, M_F)$$

- $F(x, M)$  are the parton distribution functions in the (anti) proton
- $D(z, M_F)$  fragmentation function into a photon ( $z = P_T(\gamma)/P_T(c)$ )
- $\sigma$  hard scattering cross section (short distance)
- $\mu, M, M_F$  renormalization/factorization (unphysical) scales

At NLO the definition of Direct vs Fragmentation becomes somehow arbitrary and depends on the unphysical parameter  $M_F$  which discriminates between the 2 regimes

---

## Isolation

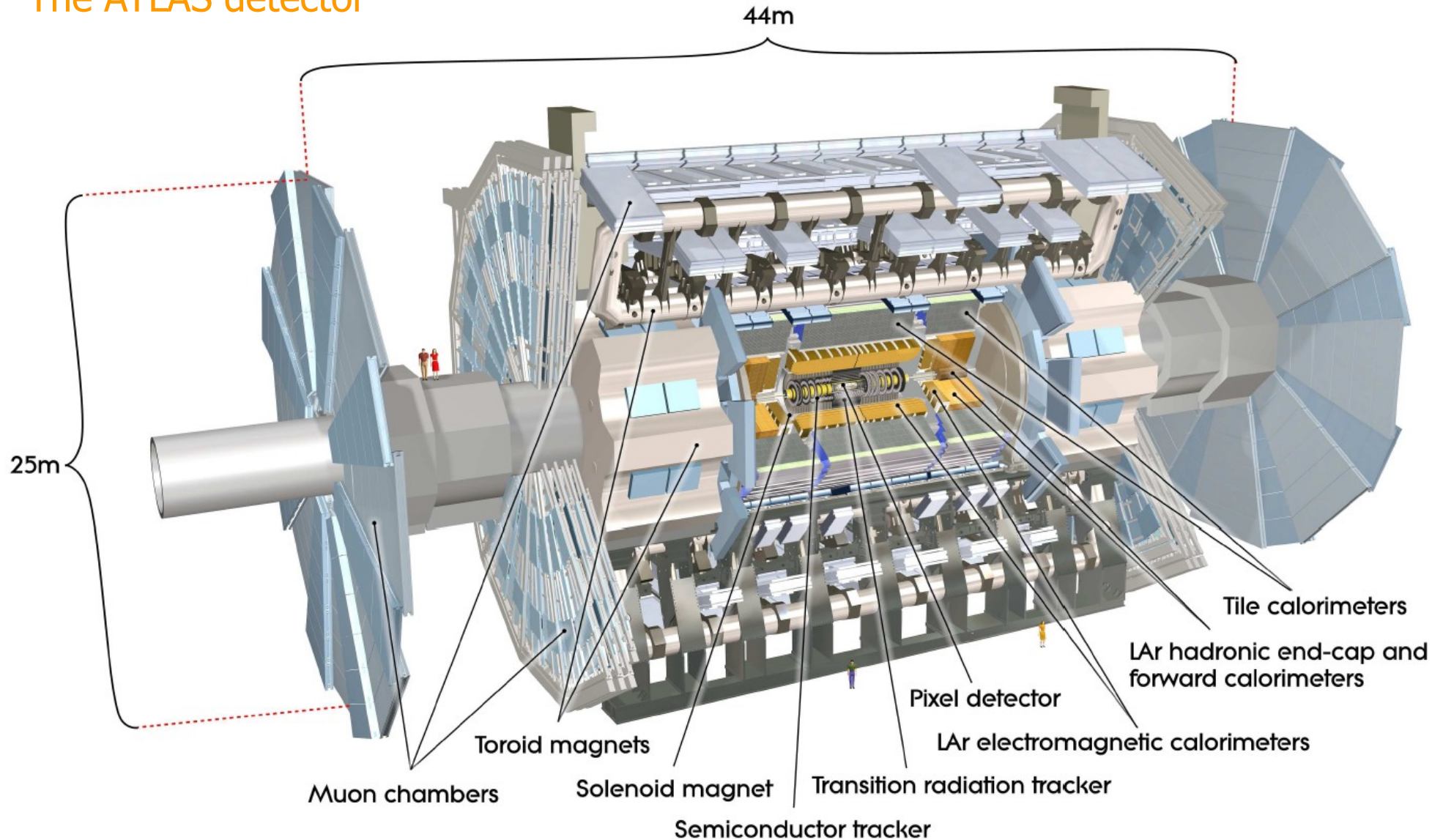
- ❑ Strictly speaking, from the experimental point of view collider experiments do not perform an *inclusive* photon measurement :
  - ❑ Background from photons coming from  $\pi^0/\eta^0$  overwhelms the signal by several order of magnitude :these are typically non isolated as mesons are usually in a jet.
  - ❑ An isolation criteria (typically a cone) is applied from the experiment side to extract the signal.
  - ❑ From the experimental point of view it is customary to define the direct photons as those which are well isolated from the hadrons in the final state while fragmentation photons as those which lie inside hadronic jets.
- ❑ From the theoretical calculation point of view, isolation can be implemented without spoiling the properties of the calculation:
  - ❑ The discrimination between direct and fragmentation based on cone isolation is not completely meaningful as it still depends on an unphysical parameter which is arbitrary: only the total cross section is a physical observable.
- ❑ A possible way to discriminate between direct/fragmentation without breaking the consistency with theory is to implement a proper isolated photon definition eg using Frixione isolation cone

---

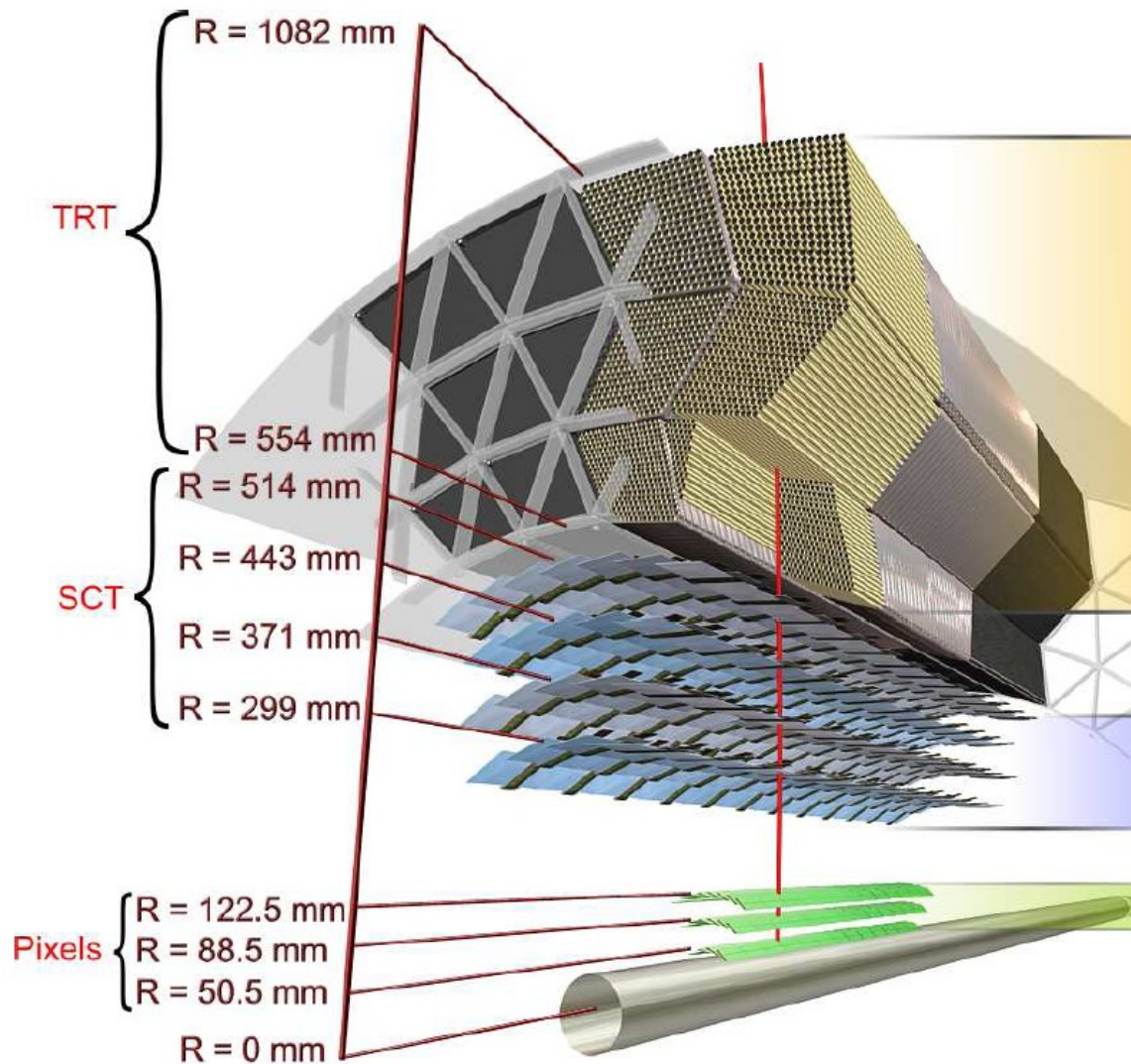
## Isolation requirements

- ❑ Maintain a high efficiency for retaining real photons while removing most of the backgrounds coming from jet fragmentation
  - ❑ want to require the isolation energy in a cone surrounding the photon be as small as possible while retaining a high (80-90%) efficiency for retaining real photons produced directly (i.e. not from fragmentation)
- ❑ Be relatively independent of the instantaneous luminosity
  - ❑ Need a dynamic definition of isolation, taking into account the instantaneous luminosity for that particular event : energy to be subtracted from the jet cone is determined by looking at either the number of reconstructed vertices for the event, or looking at the  $p_T$  density for soft jet production
- ❑ Be relatively independent of the photon energy
  - ❑ Isolation energy has to increase for high  $p_T$  photons since there is a leakage outside of the cluster. This allows additional energy to be anywhere inside the isolation cone, while the *extra* photon energy will be close to the original cluster.
- ❑ Match to perturbative predictions
  - ❑ Cone isolation is perfectly fine but the parameters have to be chosen carefully in order to preserve consistency with the theory: cone size not too small ( $R \sim 0.4/0.5$  fine) and energy in the cone not too small (few %?).

# The ATLAS detector



## Inner Detector



❑ Inner Detector (ID) is immersed in a 2 T solenoidal B-field

❑ Transition Radiation Tracker

- ❑ 350k channel tracker
- ❑ 4mm (diameter) straws
- ❑ TR detection:  $e/\pi^\pm$  discrimination
- ❑ 36 hits on track
- ❑  $130\mu\text{m}$  resolution

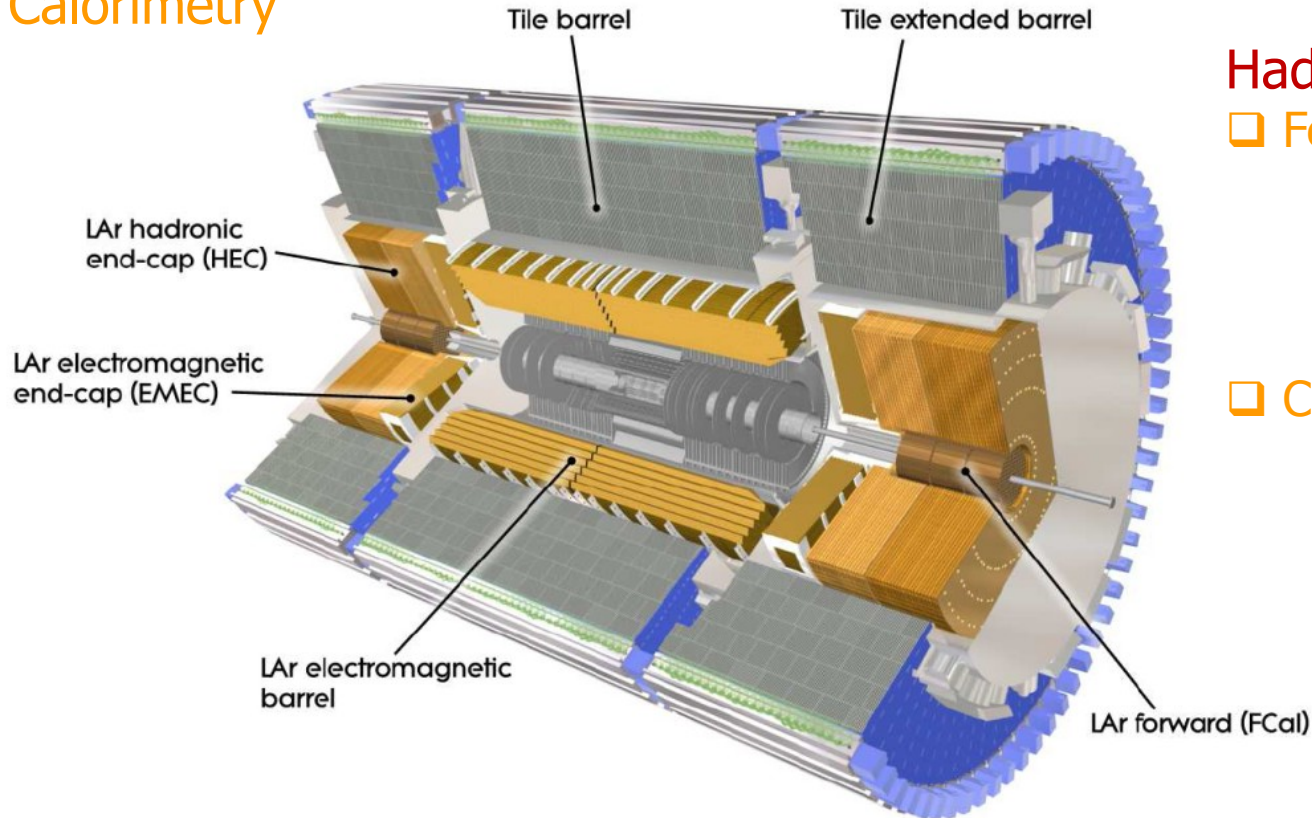
❑ Semi-Conductor Tracker

- ❑ 6.3M channels
- ❑ 4 cylinders, 8 hits/track
- ❑  $17\mu\text{m}$  resolution

❑ Pixel Tracker

- ❑ 80M channels, 3 layers
- ❑  $10\mu\text{m}$  resolution

# Calorimetry



## Hadronic Calorimeter

- ❑ Fe-scintillator for  $|\eta| < 1.7$  :
  - ❑  $\sigma(E)/E = (50\%) / \sqrt{E} \oplus 3\%$
  - ❑  $0.1 \times 0.1$  typical granularity
  - ❑ Longitudinally segmented
- ❑ Cu-LAr for  $1.5 < |\eta| < 3.2$  :
  - ❑  $\sigma(E)/E = (50\%) / \sqrt{E} \oplus 6\%$
  - ❑  $0.1 \times 0.1$  typical granularity
  - ❑ Longitudinally segmented

## Liquid Argon-Lead sampling EM calorimeter with an 'accordion' geometry :

- ❑ 3 longitudinal layers with cell of  $\Delta\eta \times \Delta\phi$ :  $(0.003-0.006) \times 0.1$  (1<sup>st</sup> layer) ;  $0.025 \times 0.025$  (2<sup>nd</sup> layer);  $0.050 \times 0.025$  (3<sup>rd</sup> layer). Allow a calo-based measurement of electron/photon direction.
- ❑ Presampler for  $|\eta| < 1.8$   $\Delta\eta \times \Delta\phi \sim 0.025 \times 0.1$
- ❑  $\sigma(E)/E = (10-17\%) (\eta) / \sqrt{E} \text{ (GeV)} \oplus 0.7\%$
- ❑ angular resolution  $50 \text{ mrad} / \sqrt{E}$  : Z vertex resolution in  $H \rightarrow \gamma\gamma$  simulated events  $\sim 16 \text{ mm}$

## Photon reconstruction

❑ Seed by a cluster in EM calorimeter with 3x5 cells in 2<sup>nd</sup> layer exceeding 2.5 GeV

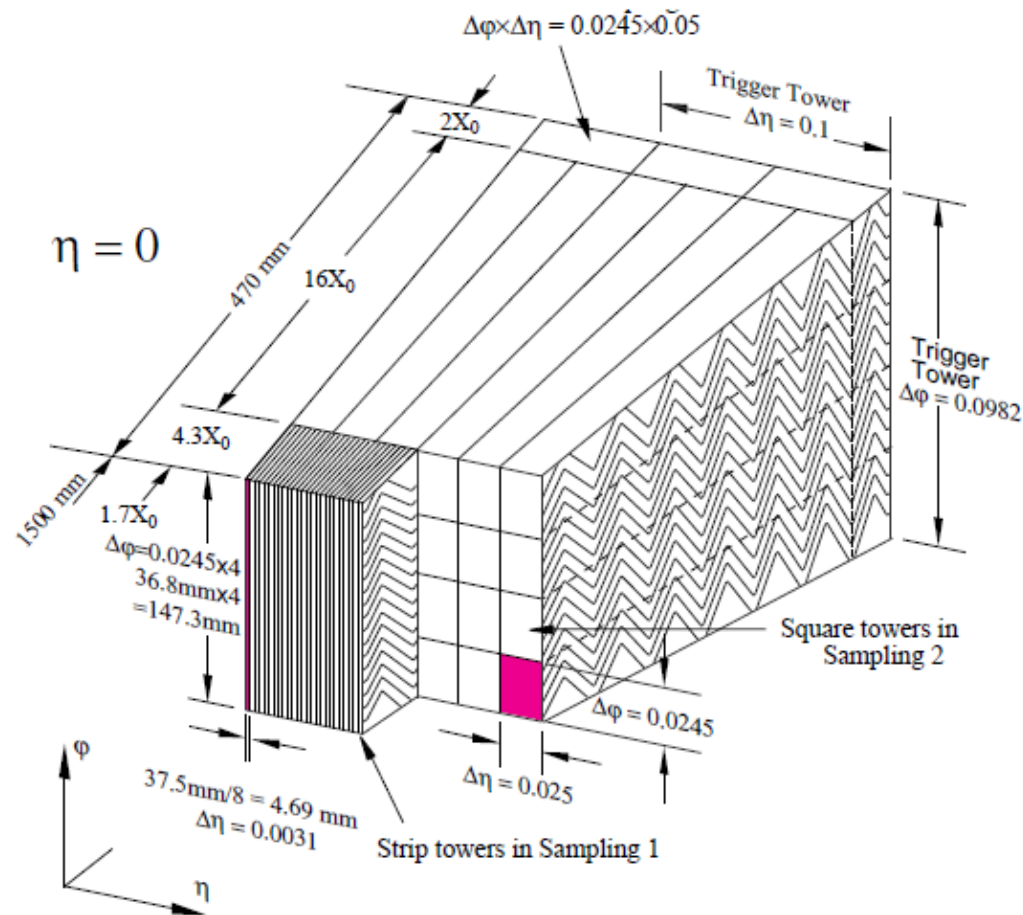
❑ Track-cluster matching :

- ❑ No matched track : unconverted  $\gamma$
- ❑ Matched to track(s) from  $\gamma$  conversion in ID : converted  $\gamma$ . Single track conversions are also retained
- ❑ Different cluster sizes for converted (3x7) and unconverted (3x5) photons (5x5 for both in the endcap)

❑ Energy : determined with EM calorimeter

- ❑ Energy calibration is optimized separately for converted and uncovered photons on Geant4 based detailed full detector simulations
- ❑ Energy scale know better than 1% from data driven studies

❑ Require pseudorapidity range covered by strips :  $|\eta| < 1.37$ ,  $1.52 < |\eta| < 2.37$  and now overlap with calorimeter dead regions (mainly for 2010 data)



# Photon identification

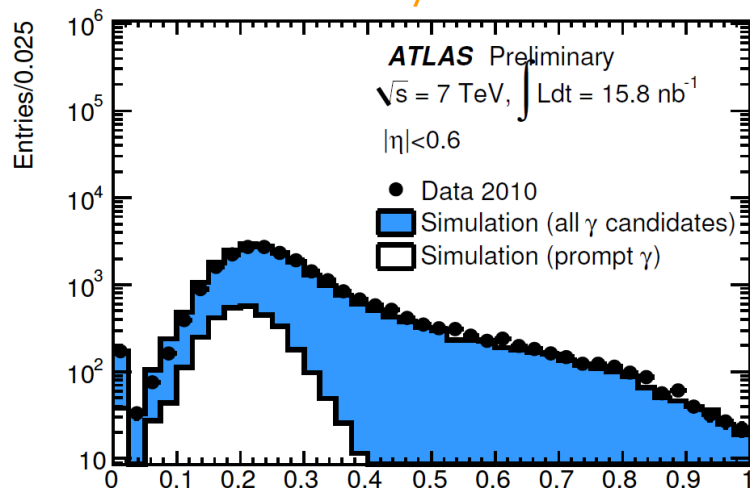
Simple cuts on shower shape variables (isEM) : 2 levels of quality are defined

## ❑ “loose” photon definition:

- ❑ leakage in the hadronic calorimeter
- ❑ second EM calorimeter sampling shower shapes

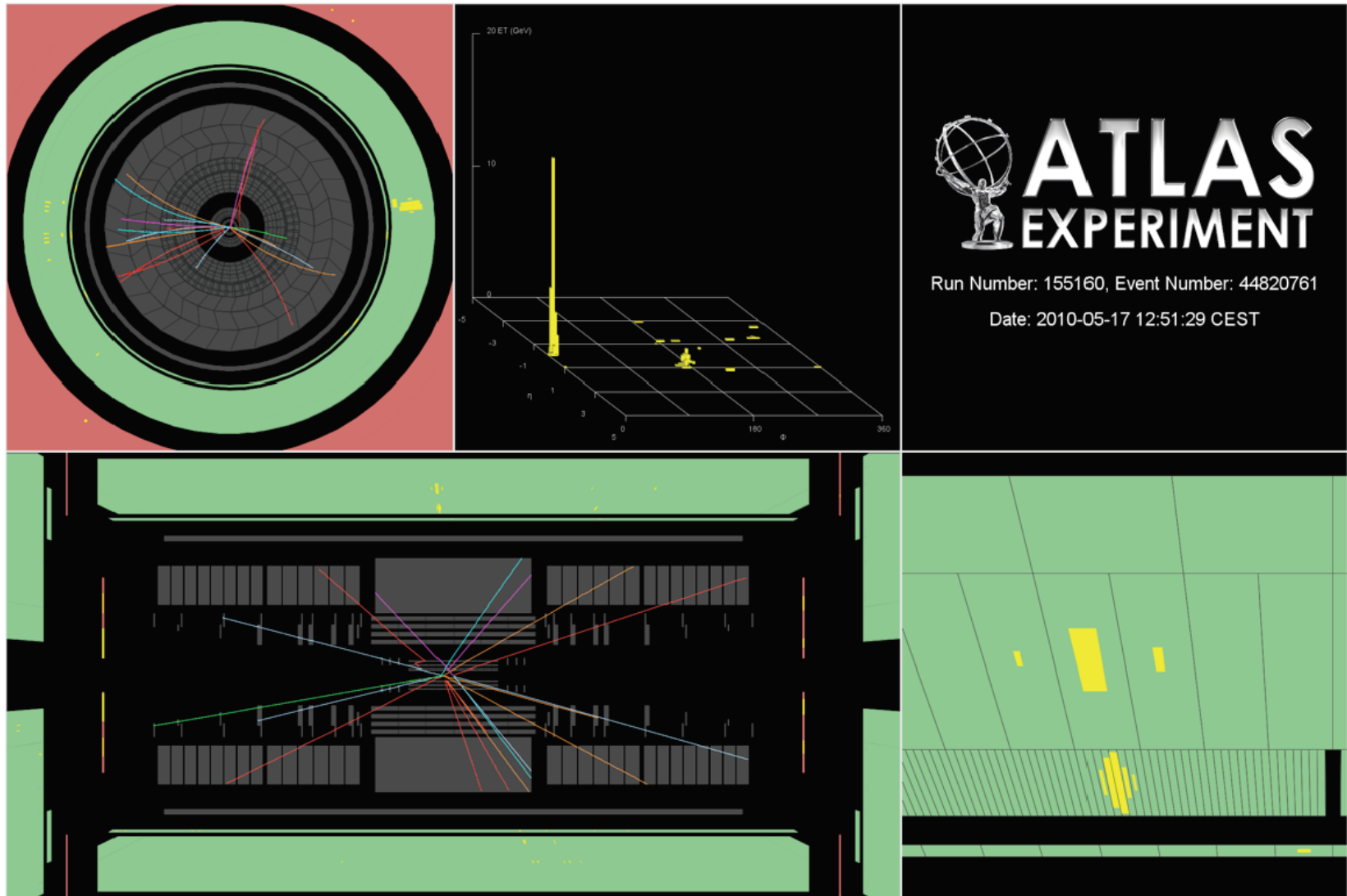
## ❑ “tight” photon definition :

- ❑ tighter cuts on the “loose” photon variables
- ❑  $R_\phi$  from 2<sup>nd</sup> sampling added
- ❑ Shower shapes cuts in the first sampling
- ❑ Different cuts for converted and unconverted photons tuned to have  $\sim$  same efficiency

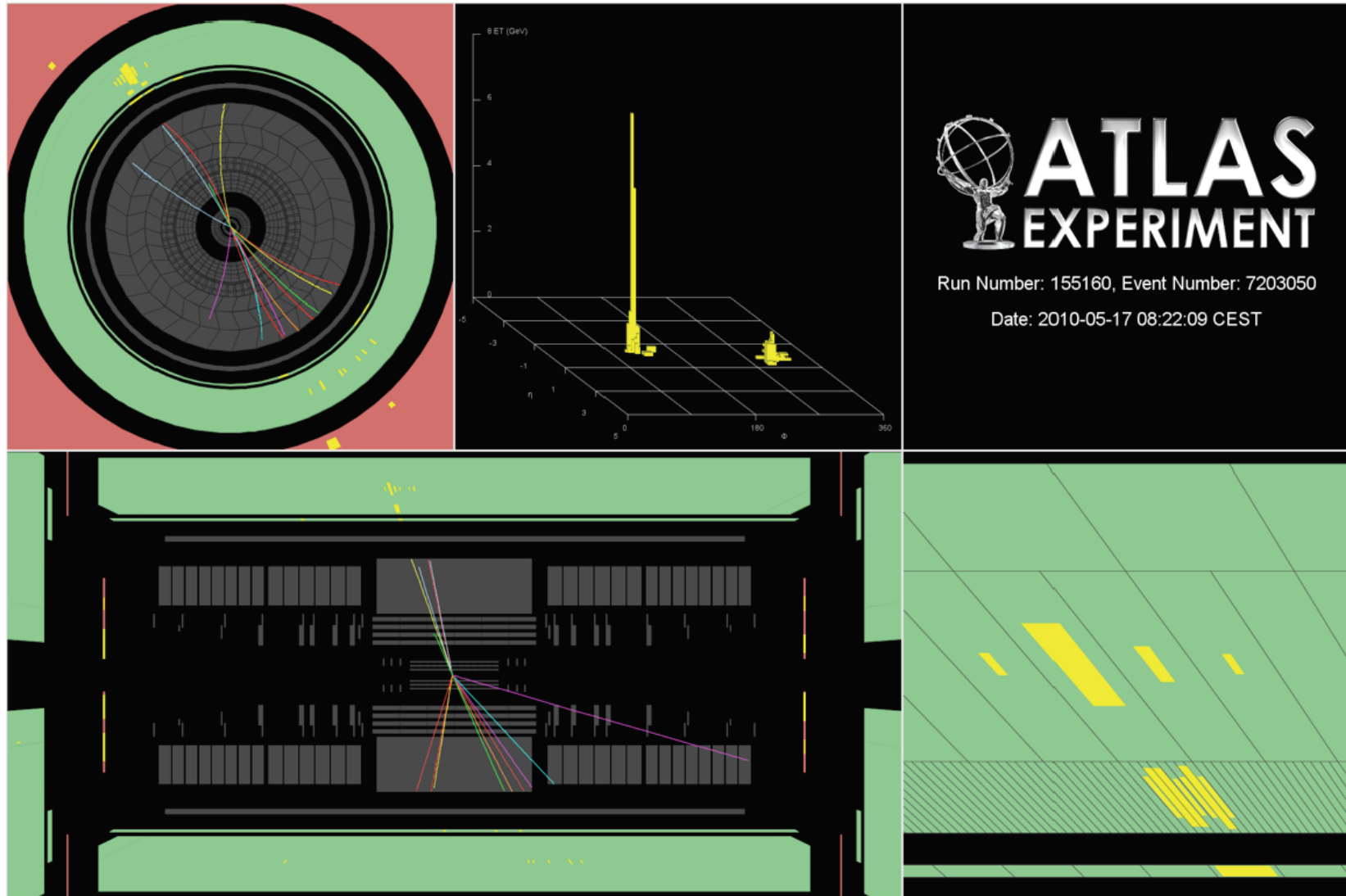


Category	Description	Name	Loose	Tight
Acceptance	$ \eta  < 2.37, 1.37 <  \eta  < 1.52$ excluded	—		✓
Hadronic leakage	Ratio of $E_T$ in the first sampling of the hadronic calorimeter to $E_T$ of the EM cluster (used over the range $ \eta  < 0.8$ and $ \eta  > 1.37$ )	$R_{had_1}$	✓	✓
	Ratio of $E_T$ in all the hadronic calorimeter to $E_T$ of the EM cluster (used over the range $ \eta  > 0.8$ and $ \eta  < 1.37$ )	$R_{had}$	✓	✓
EM Middle layer	Ratio in $\eta$ of cell energies in $3 \times 7$ versus $7 \times 7$ cells	$R_\eta$	✓	✓
	Lateral width of the shower	$w_2$	✓	✓
	Ratio in $\phi$ of cell energies in $3 \times 3$ and $3 \times 7$ cells	$R_\phi$		✓
EM Strip layer	Shower width for three strips around maximum strip	$w_{s3}$		✓
	Total lateral shower width	$w_{stot}$		✓
	Fraction of energy outside core of three central strips but within seven strips	$F_{side}$		✓
	Difference between the energy of the strip with the second largest energy deposit and the energy of the strip with the smallest energy deposit between the two leading strips	$\Delta E$		✓
	Ratio of the energy difference associated with the largest and second largest energy deposits over the sum of these energies	$E_{ratio}$		✓

## A nice photon candidate



## A nice fake photon candidate



## Photon isolation

Isolation is necessary to get rid of the jet background and (to some extent) of the fragmentation contribution: the definition of the isolation prescription is a tricky business

### ❑ Calorimeter isolation

- ❑ Based on sum of energies in cells in cone  $R < 0.4$  in  $\eta$ - $\phi$  around the photon, removing the cells in a  $5 \times 7$  cluster

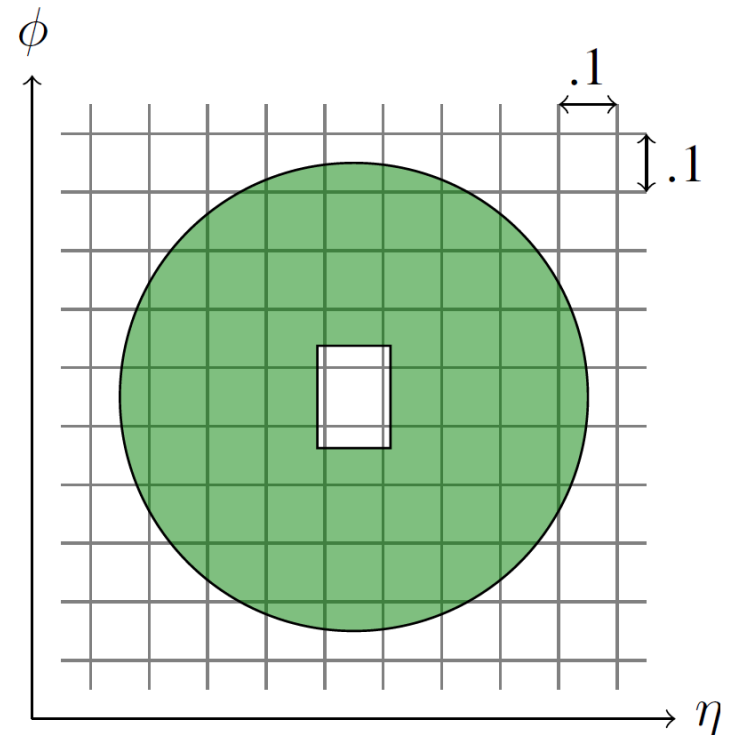
### ❑ Corrections for residual leakage of photon energy, using single photon MC samples

- ❑  $P_T$  dependence removed correcting with coefficients from single particles full simulation.

### ❑ Corrections for non perturbative effects (underlying event, pileup)

- ❑ Using ambient energy density estimated with low- $p_T$  jets, following M. Cacciari, G. P. Salam, S. Sapeta,

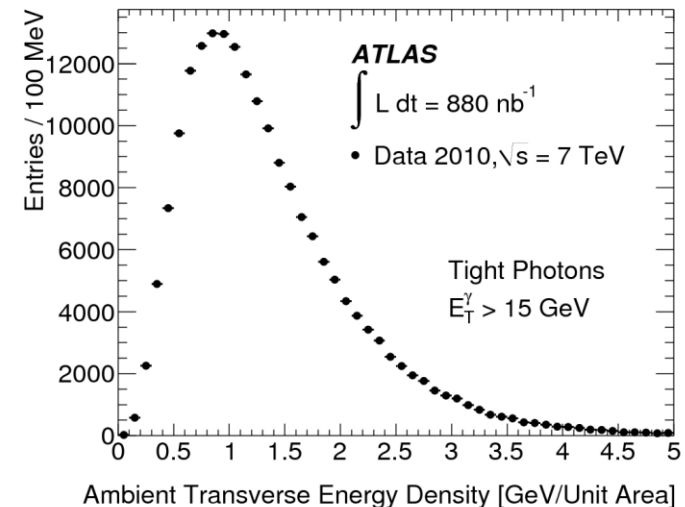
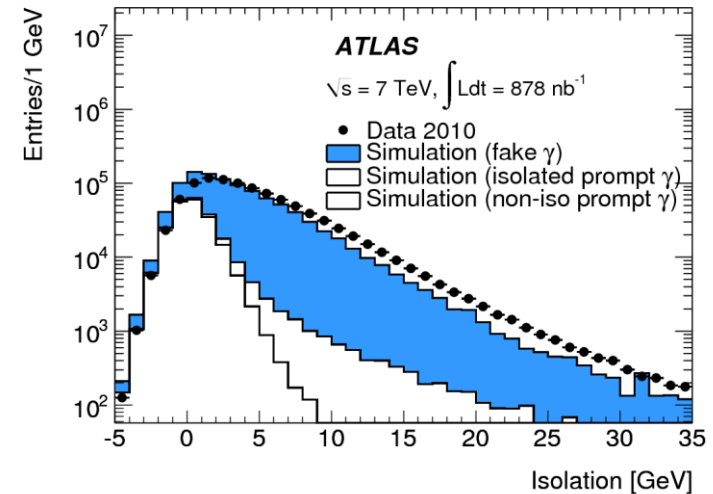
(<http://arxiv.org/abs/0912.4926>)



## Photon isolation

Ambient energy density is estimated event by event using low  $P_T$  jets :

- ❑ Run jet finding kT algorithm, with minimum  $P_T$  at 0, to allow for very soft objects
- ❑ Compute Voronoi areas of jets (partitioning the  $(\eta, \phi)$  space into regions defined by nearest jet)
- ❑ From the jets and their areas, find the median energy density for the bin. Median helps to avoid any scale effects from setting an upper bound on jet  $P_T$
- ❑ For events with low multiplicity and hard interactions, can remove  $n$  most energetic jets from event (where  $n$  is typically 2). Correction to isolation variables made based on the cone size



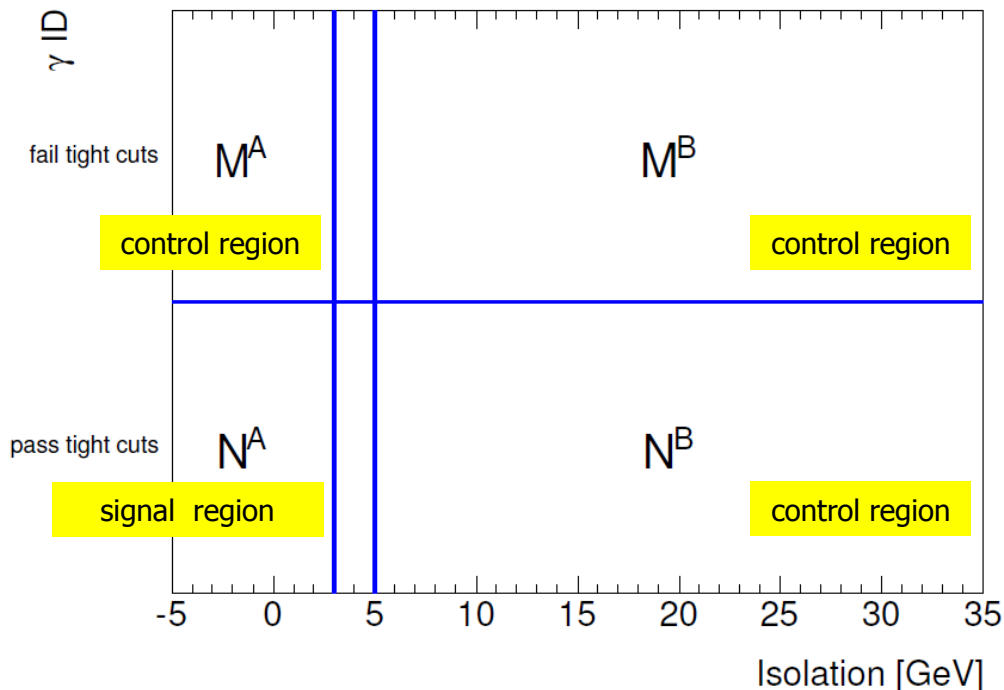
## Signal extraction :

Data driven approaches : a 2D-sidebands subtraction and an isolation template fit (a la CDF) and a method:

- ❑ A 2D histogram is built: (tight-4 strips) variable on one axis and calorimetric isolation on the other. 2 assumptions
- ❑ No correlation between isolation and isEM for the background
- ❑ No signal in the control regions

$$N_{\text{sig}}^A = N^A - N^B \frac{M^A}{M^B}$$

$$P = 1 - \frac{N^B}{N^A} \frac{M^A}{M^B}$$



### ❑ Signal region (N<sup>A</sup>):

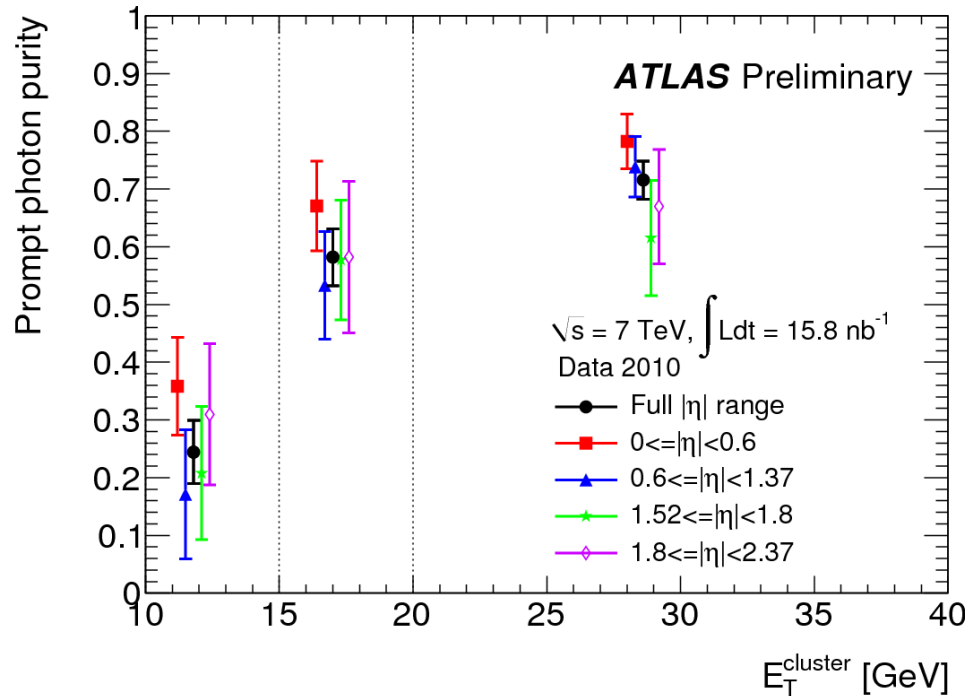
- ❑ Calo isolation < 3 GeV; pass tight photon selection

### ❑ Bkg control regions:

- ❑ non-isolated (N<sup>B</sup>): Calo isolation ≥ 5 GeV, pass tight photon selection
- ❑ non-tight-ID (M<sup>A</sup>): Calo isolation < 3 GeV, fail tight photon selection, pass tight photon selection after relaxing fracm, weta1, DeltaE, Eratio
- ❑ non-isolated and non-tight-ID (M<sup>B</sup>): Calo isolation ≥ 5 GeV, fail tight photon selection, pass tight photon selection after relaxing fracm, weta1, DeltaE, Eratio

# Evidence of direct photons in very first data

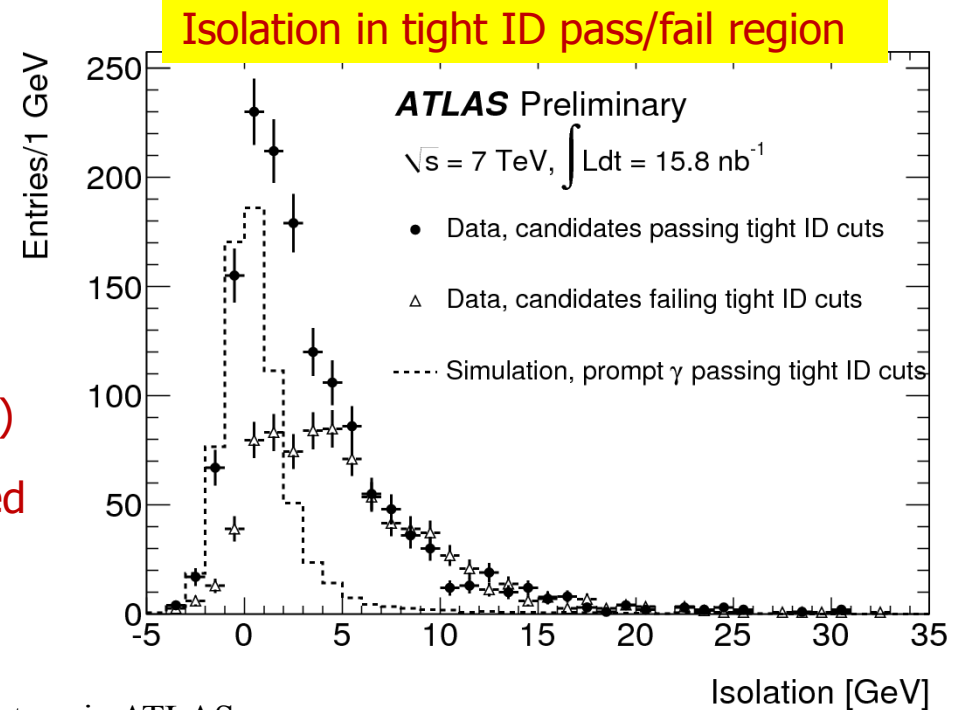
ATLAS-CONF-2010-077



□ Data candidates failing the tight ID cuts distribution normalized by the ratio  $N^B/M^B$  (same number of events in the non isolated control region)

□ MC signal distribution normalized to the estimated yield in data in the signal region (divided by the expected efficiency of the isolation criterium)

First evidence of prompt photon signal in ATLAS: a clear excess can be observed and is consistent with the expected shape for from MC.



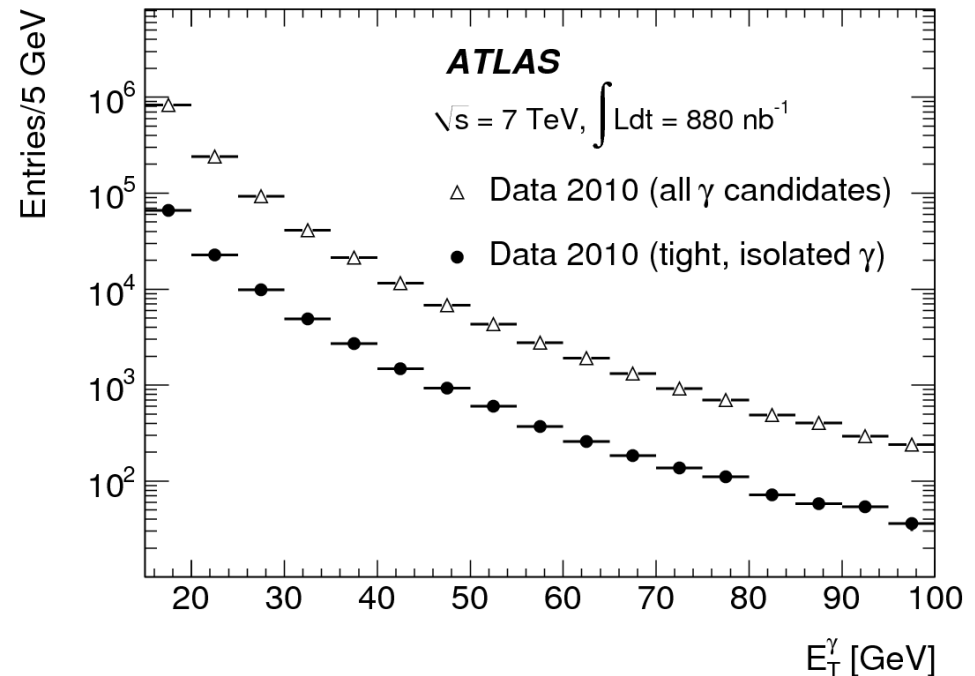
## Inclusive photon cross section : preselection

Two analysis with different integrated luminosity (very similar ingredients) :

- ❑ **Phys. Rev. D 83, 052005 (2011)**:  $880 \text{ nb}^{-1}$ , from 15 GeV to 100 GeV, 3 eta bins  $[0.00, 0.60)$ ,  $[0.60, 1.37)$ ,  $[1.52, 1.81)$
- ❑ **ATLAS-CONF-2011-058** :  $37 \text{ pb}^{-1}$ , from 45 GeV to 400 GeV, 4 eta bins  $[0.00, 0.60)$ ,  $[0.60, 1.37)$ ,  $[1.52, 1.81)$ ,  $[1.81, 2.37)$

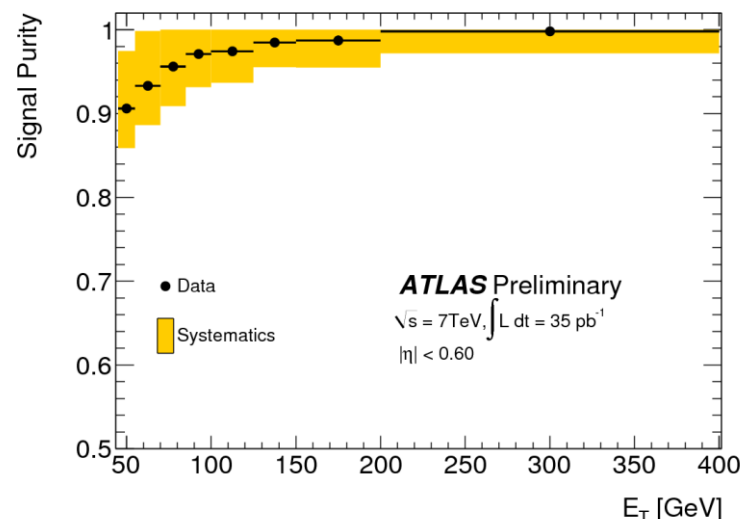
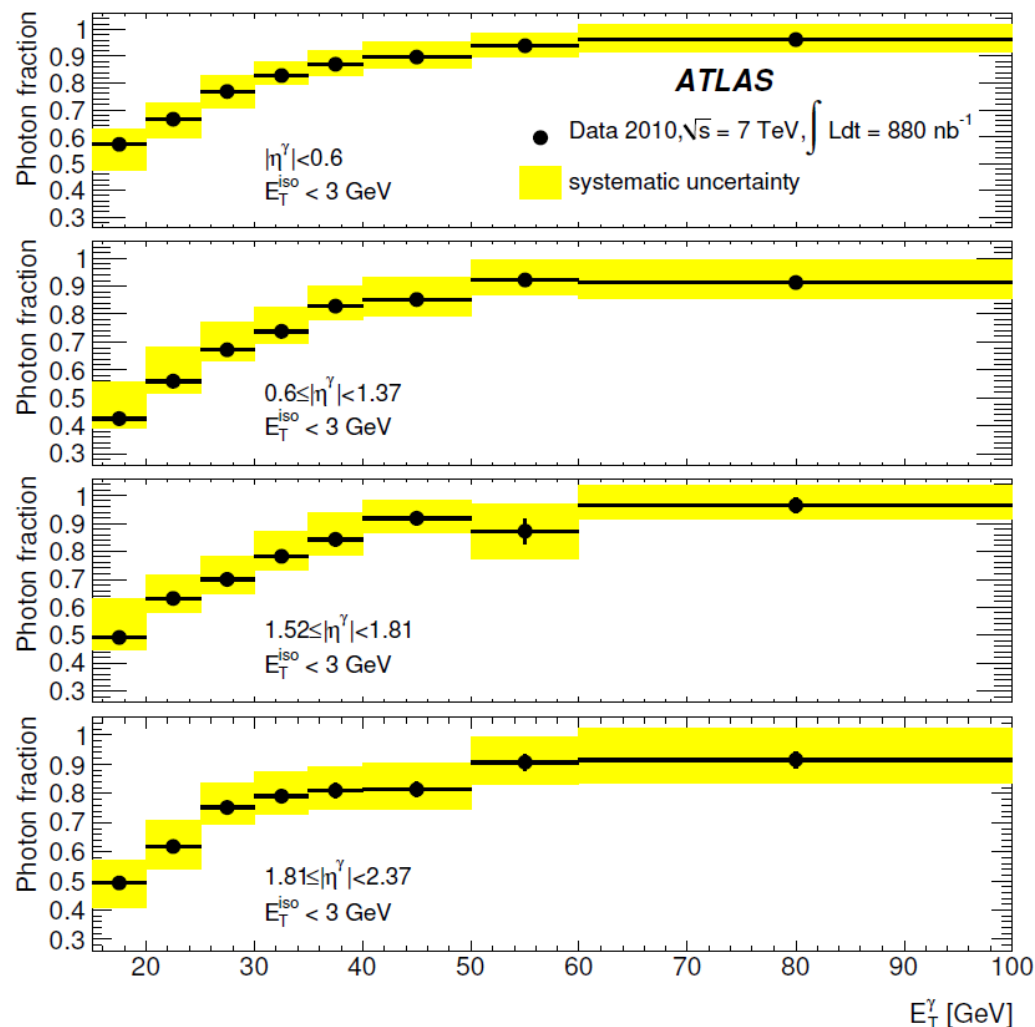
## Event selection :

- A. Event is in the standard GoodRunList (tracker and calorimeters fully operational)
- B. Event passes a loose 10 GeV threshold ( $880 \text{ nb}^{-1}$ ) and 40 GeV ( $37 \text{ pb}^{-1}$ ) trigger
- C. The primary vertex has at least 3 tracks
- D. The photon candidate passes the e/gamma object quality (OQ) cuts (avoid overlap with faulty calorimeter regions)
- E. The photon candidate passes the tight cuts
- F. The photon has a corrected isolation energy less than 3 GeV in a 0.4 cone
- G. 110K (15-100 GeV,  $|\eta| < 1.81$ ,  $0.9 \text{ pb}^{-1}$ ),  
174K (45-400 GeV,  $|\eta| < 2.37$ ,  $35 \text{ pb}^{-1}$ )



## Photon purity estimation :

Photon purity rapidly increases from 50% (15 GeV) to >95% above 100 GeV



- ❑ Main systematic uncertainties from: MC inputs (up to ~10%); background control regions (up to 6%)
- ❑ Results cross-checked with isolation template fit (signal template: e from W/Z in data; bkg template: photons failing the tight ID criteria)
- ❑ The results from 2D sidebands method and full isolation template fit agree within 5%

---

## Photon efficiency

Here we start playing a difficult game : the key point is that we do not have yet a sizeable clean source of photons to extract in a purely data-driven way the photon efficiency.

- ❑ Need to accept some (reasonable) compromises: use the MC, check whatever can be done on data and assign proper systematic uncertainty
- ❑ Compare the shower shapes used to identify photons in data and MC : correct the photon shapes in MC to match the data and compute 'corrected' efficiencies
  - ❑ typically showers are slightly larger ( $\sim\%$  level) in data than in MC (also seen on electrons)
  - ❑ a mixture of true photon and jets (purity is not 100%) so a systematic uncertainty has to be assigned
- ❑ Infer photon behavior from pure sample of electrons and use the MC to assess the differences:
  - ❑ converted photons have a similar shower development in the calorimeter so the photon efficiency for converted photons can be estimated  $\sim$  directly from electrons
  - ❑ unconverted photon shapes are very different from the electrons one, not straightforward
- ❑ Use photons from  $Z \rightarrow \mu\mu\gamma$  and  $Z \rightarrow \tau\tau\gamma$  to measure the photon efficiency for low  $p_T$  (need  $> \text{fb}^{-1}$  (start to be appealing))

## Photon efficiency

❑ Photon reconstruction/acceptance efficiency  $\sim 80\text{-}85\%$  in the barrel ( $|\eta| < 1.37$ ),  $\sim 75\%$  in the endcap ( $1.52 < |\eta| < 2.37$ )

❑ significant part of inefficiency (dead readout) recovered in 2011 winter shutdown

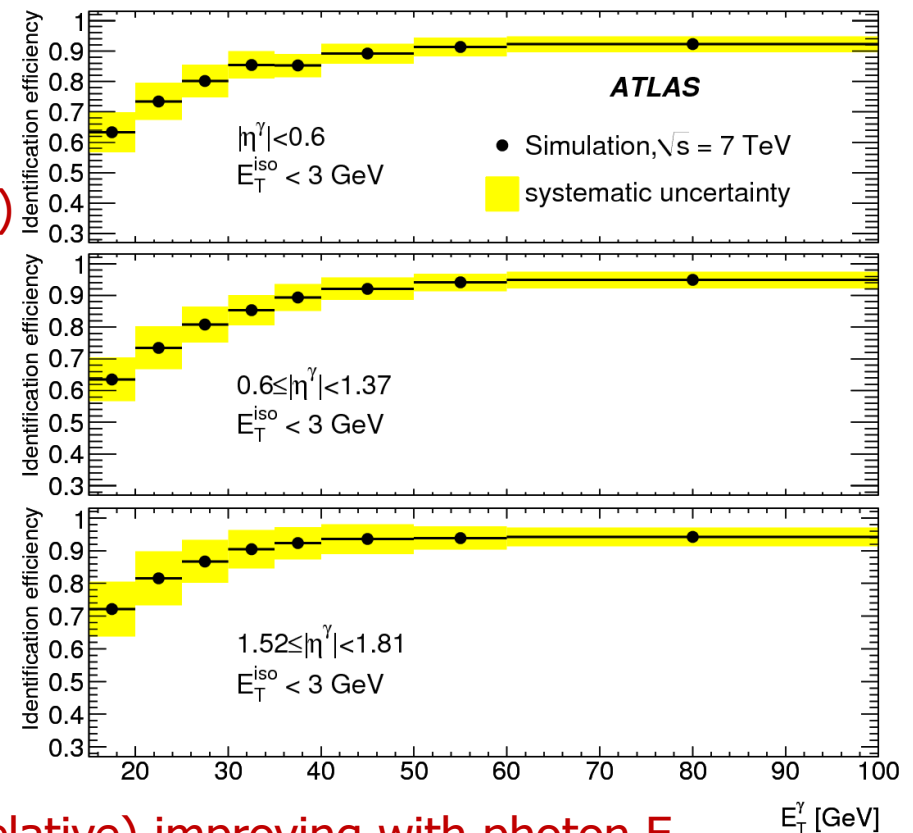
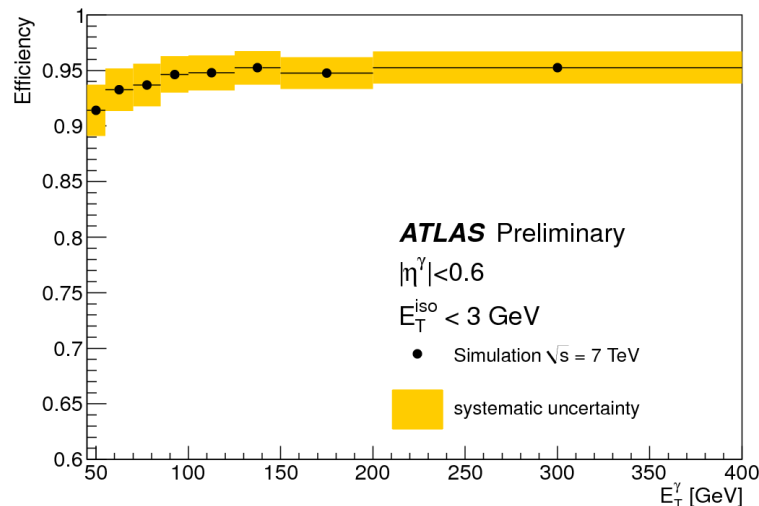
❑ Photon identification efficiency from MC. Main systematic uncertainties:

❑ method, selection ( $\approx 5\% \rightarrow 2\%$ )

❑ extra material ( $\approx 6\% \rightarrow 1\%$ )

❑ pileup, generator ( $\approx 2\text{-}3\%$ )

❑ Trigger efficiency  $\sim 99.5\%$  ( $\sim 1\%$  uncertainty)



Overall systematic uncertainty from 15% (relative) improving with photon  $E_T$

---

## Cross section and comparison with theoretical predictions

Theoretical predictions obtained with JETPHOX (NLO montecarlo which includes a consistent treatment of the fragmentation contribution) using CTEQ6.6 (MSTW 2008 3-5% difference).

❑ Same kinematic cut and pseudo isolation (at the parton level) isolation to mimic the experimental isolation is implemented :

❑ require  $E_T < 4$  GeV in a cone of 0.4 around the candidate

❑ Systematic uncertainties evaluated in a rather conventional way by

❑ varying PDF eigenvalues (4% to 2%)

❑ varying scales from  $P_{T^\gamma}/2$  to  $2 \cdot P_{T^\gamma}$  (20% to 8%) (independently, to avoid accidental cancellations)

❑ parton isolation cut varied from 2 to 6 GeV (2%)

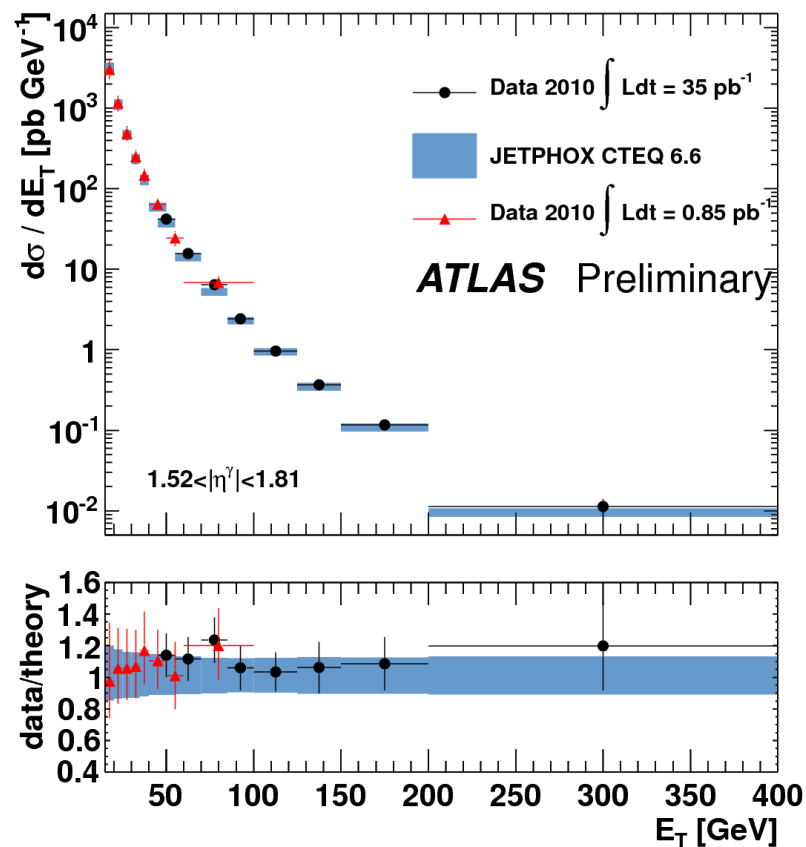
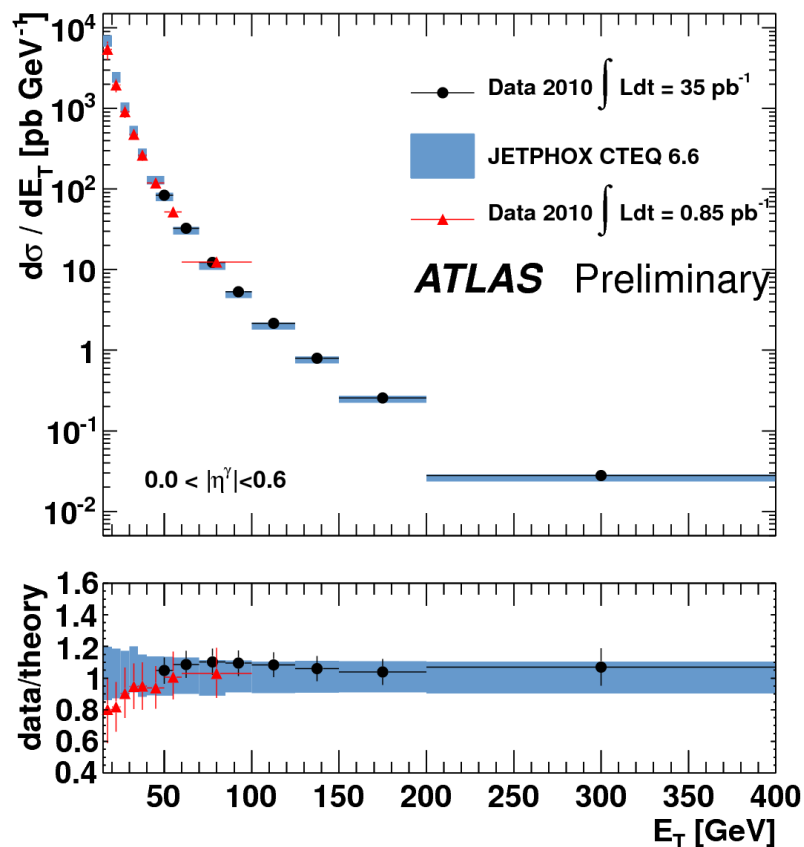
## Additional systematic uncertainty for the measurement

❑ Luminosity uncertainty 11% down to 3.5%

❑ Photon energy scale systematic uncertainty : 3% (leading to 10% on the cross section) in the 880 nb<sup>-1</sup> analysis and 1.5% (leading to 5% on the cross section)

❑ Bin by bin unfolding wrt to Bayesian < 2% difference

## Data-Theory comparison



Results systematically limited across full  $E_T$  range

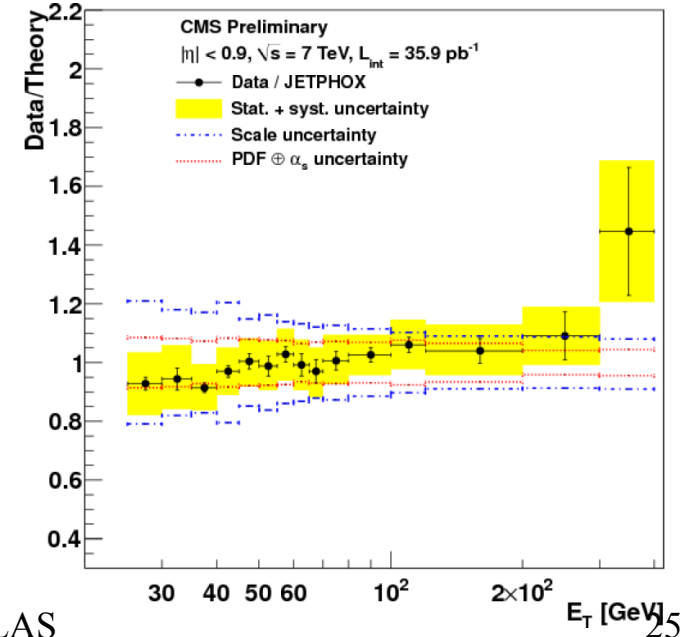
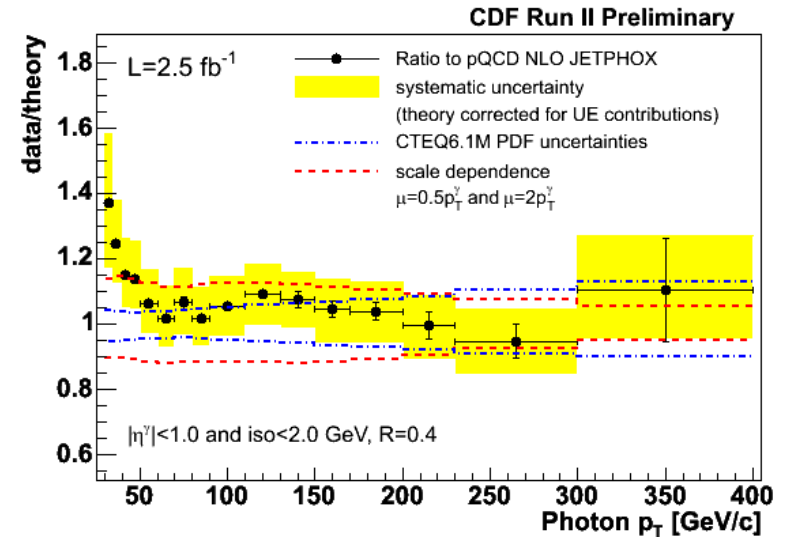
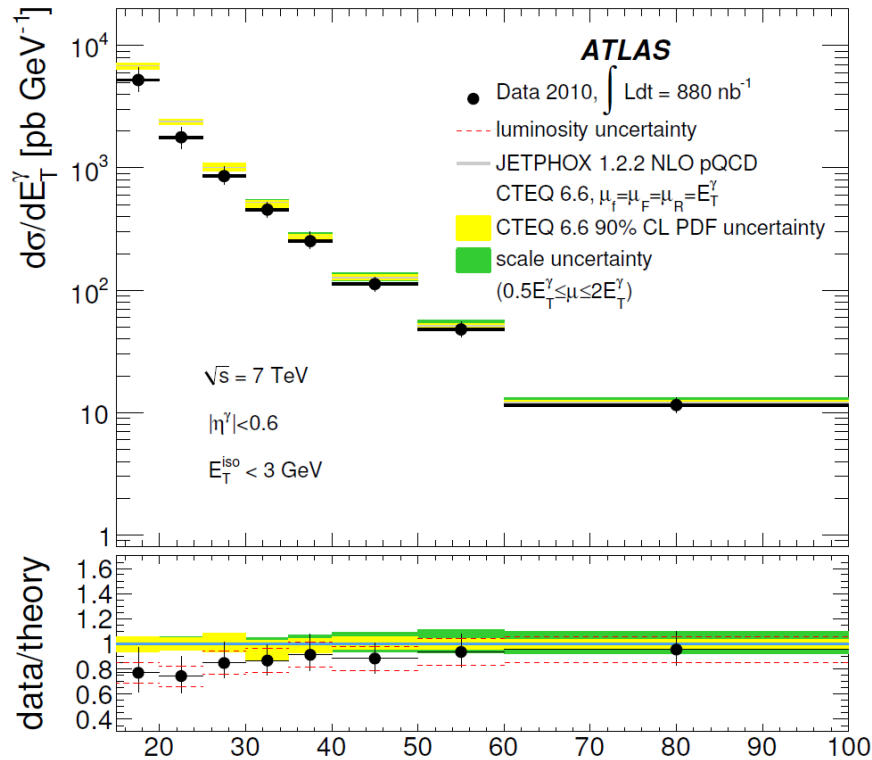
❑ The two measurements are consistent in the overlapping  $E_T, \eta$  bins

❑ Data/(NLO pQCD) comparison:

❑ experimental uncertainty comparable to theoretical one

❑ disagreement (ratio data/theory < 1) below 35 GeV in the central region, good agreement above

## data/theory comparison in other experiments



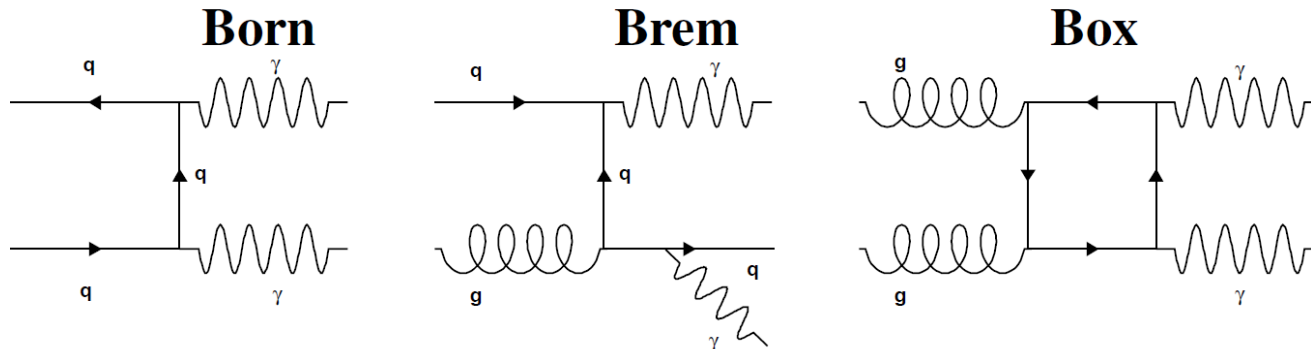
❑ Around 30 GeV both ATLAS and CMS report a slight deficit wrt to theory while CDF a sizeable excess (although x is different!)

❑ sizeable deficit reported by ATLAS in the very low  $E_T$  region ( $\sim 15 \text{ GeV}$ )

❑ all experiments show a good agreement from 50 GeV

## Di-photon production cross section

- ❑ The measurement of the di-photon production cross section at the LHC is again an important probe of our understanding of the QCD especially in some kinematic regions
  - ❑ the  $\Delta\phi$  separation between the photons is sensitive to the way the double fragmentation is modelled
  - ❑ the balanced back to back case ( $\Delta\phi \sim \pi$  and small total  $P_T$ ) is sensitive to the soft gluon emission



- ❑ Di-photon signature appears in some 'new physics' processes :
  - ❑ irreducible background for Higgs decay into 2 photons
  - ❑ non resonant production associated with significant MET is predicted by UED/SUSY models
  - ❑ a narrow resonance at high mass predicted by extra dimensions models
- ❑ Main ingredients similar to the inclusive analysis : 3 methods to extract the signal yield from data in a purely data-driven way

## Background subtraction (I) : event weighting method

❑ This is a technique used already by CDF and D0 :


- ❑ define a cut on your photon candidates which characterize your signal :  $E_{\text{isol}}^T < 3 \text{ GeV}$
- ❑ classify the di-photon events candidates in 4 categories. PP/PF/FP/FF : these numbers are related connected the true number of  $\gamma\gamma/\gamma\text{-jet}/\text{jet-}\gamma/\text{jet-jet}$  by an efficiency matrix

$$\begin{pmatrix} S_{\text{PP}} \\ S_{\text{PF}} \\ S_{\text{FP}} \\ S_{\text{FF}} \end{pmatrix} = \mathbf{E} \begin{pmatrix} W_{\gamma\gamma} \\ W_{\gamma j} \\ W_{j\gamma} \\ W_{jj} \end{pmatrix}$$

❑  $\epsilon$  and  $f$  are the probabilities for a true and fake photon respectively to pass the isolation cut.  $\epsilon$  is typically 80 to 95% while  $f \sim$  from 20 to 40 %

❑ the key point here is that these efficiencies are measured on data from the tight/non-tight isolation distributions

❑ Actually the true efficiency matrix is a bit more complicated as there's some correlation in the FF case



$$\begin{pmatrix} \epsilon_1 \epsilon_2 & \epsilon_1 f_2 & f_1 \epsilon_2 & f_1 f_2 \\ \epsilon_1 (1 - \epsilon_2) & \epsilon_1 (1 - f_2) & f_1 (1 - \epsilon_2) & f_1 (1 - f_2) \\ (1 - \epsilon_1) \epsilon_2 & (1 - \epsilon_1) f_2 & (1 - f_1) \epsilon_2 & (1 - f_1) f_2 \\ (1 - \epsilon_1)(1 - \epsilon_2) & (1 - \epsilon_1)(1 - f_2) & (1 - f_1)(1 - \epsilon_2) & (1 - f_1)(1 - f_2) \end{pmatrix}$$

## Background subtraction (II) : the 2D sidebands method extension

Extend the 2D sidebands method to the case of 2 photon candidates :

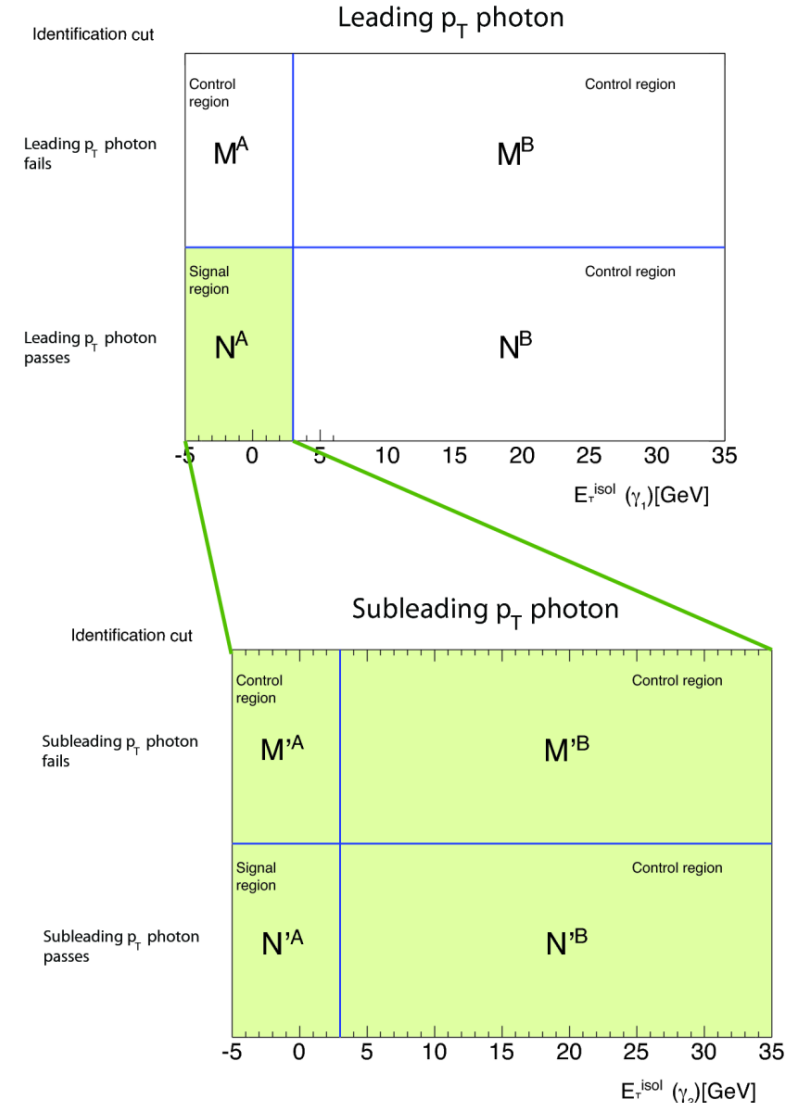
- ❑ preselect events with 2 candidates passing a loose photon definition.
- ❑ As for the inclusive analysis the number of signal candidates in region A of the first matrix is

$$N_A^{\text{sig}} = N_A - \left[ (N_B - c_1 N_A^{\text{sig}}) \frac{N_C - c_2 N_A^{\text{sig}}}{N_D - c_1 c_2 N_A^{\text{sig}}} \right] R^{\text{bkg}}$$

- ❑ For events with the leading candidates in A region a second 2D matrix is used for the second candidate
- ❑ After a bit of algebra

$$N_{\gamma\gamma}^{\text{TITI}} = \frac{\epsilon' \left( \alpha f' N_A^{\text{sig}} + (\alpha - 1) N_A'^{\text{sig}} \right)}{(\alpha - 1) \epsilon' + \alpha f'}$$

( $\alpha$  has to be taken from MC while the other parameters from data)



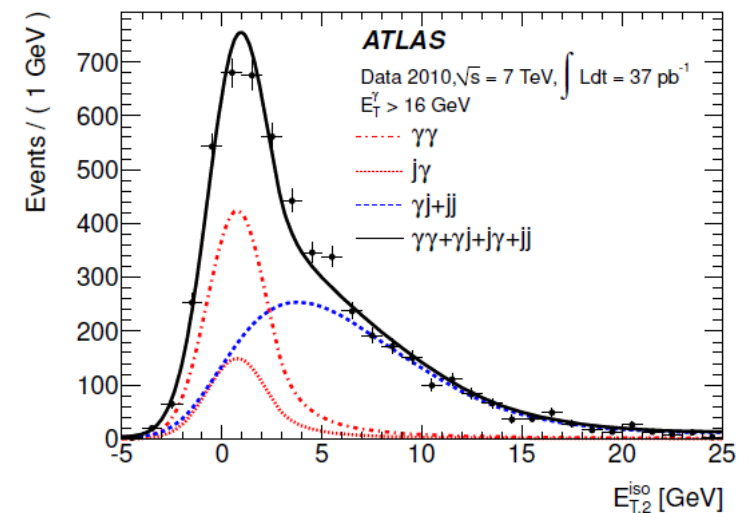
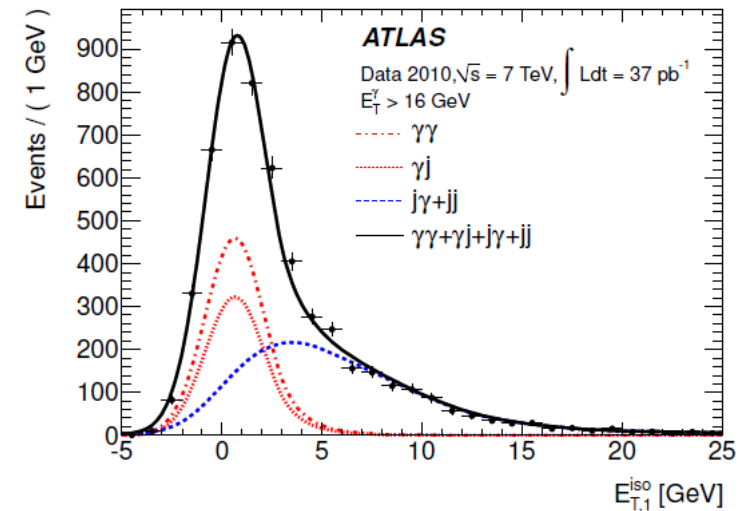
## Background subtraction (III) : the 2D sidebands method extension

For all events with 2 photon candidates passing the tight isolation criteria

- ❑ isolation templates for  $\gamma\gamma$ ,  $\gamma$ -j and jet-jet events are built from data (using electrons and the non-tight sample)
- ❑ the 2D distribution of the leading and subleading photon is built
- ❑ the sample decomposition comes from a maximum likelihood fit

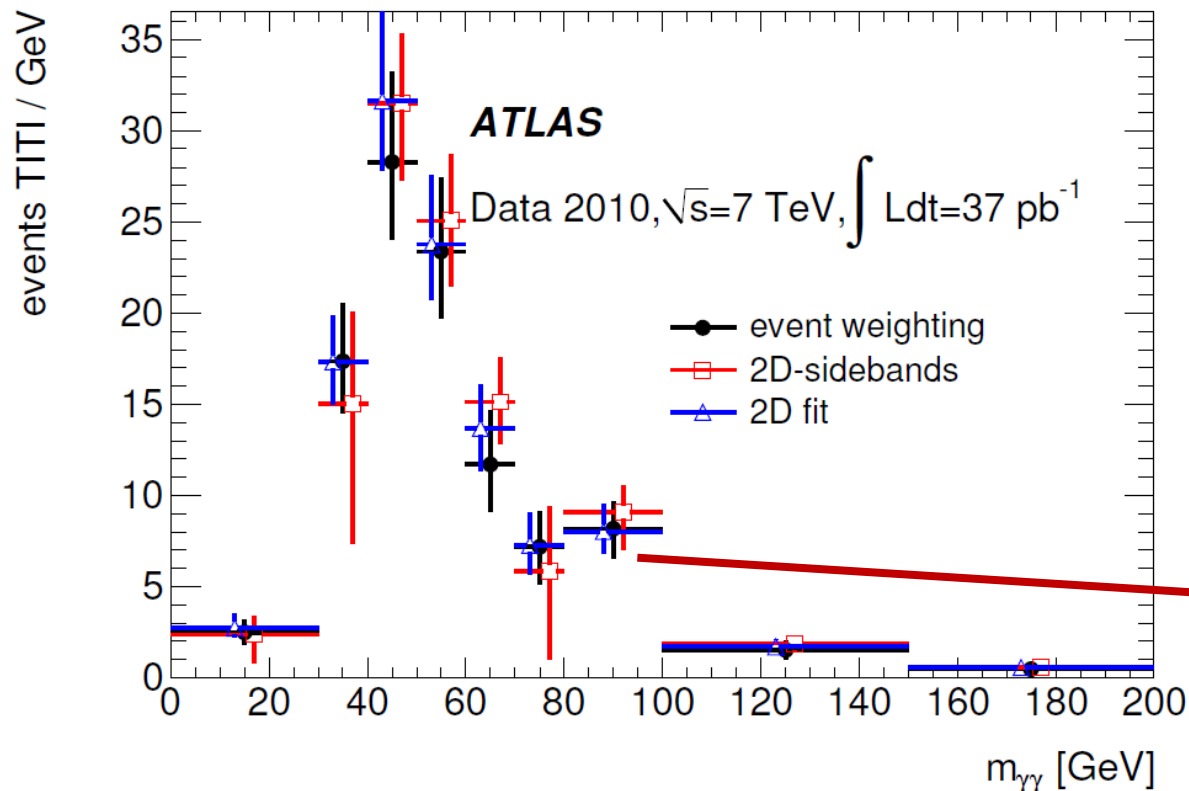
$$\begin{aligned}
 N^{\text{TT}} F^{\text{obs}}(E_{\text{T},1}^{\text{iso}}, E_{\text{T},2}^{\text{iso}}) = & N_{\gamma\gamma}^{\text{TT}} F_{\gamma_1}(E_{\text{T},1}^{\text{iso}}) F_{\gamma_2}(E_{\text{T},2}^{\text{iso}}) \\
 & + N_{\gamma j}^{\text{TT}} F_{\gamma_1}(E_{\text{T},1}^{\text{iso}}) F_{j_2}(E_{\text{T},2}^{\text{iso}}) \\
 & + N_{j\gamma}^{\text{TT}} F_{j_1}(E_{\text{T},1}^{\text{iso}}) F_{\gamma_2}(E_{\text{T},2}^{\text{iso}}) \\
 & + N_{jj}^{\text{TT}} F_{jj}(E_{\text{T},1}^{\text{iso}}, E_{\text{T},2}^{\text{iso}})
 \end{aligned}$$

- ❑ due to correlations the jet-jet case can't be factorized

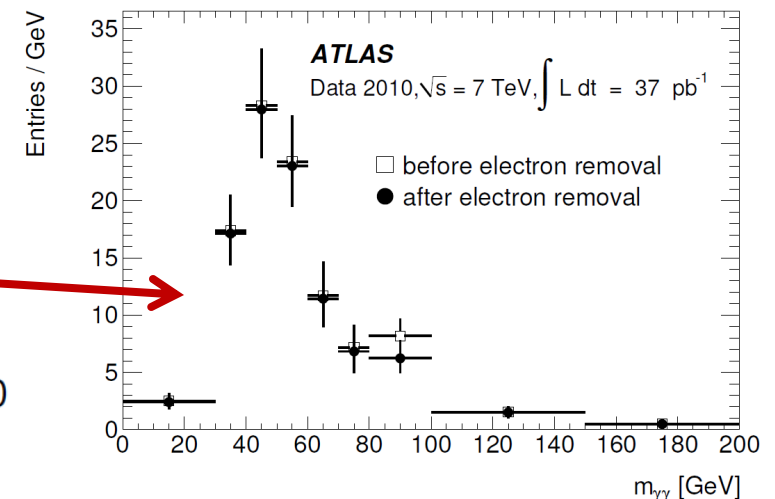


## Extracting the signal yield

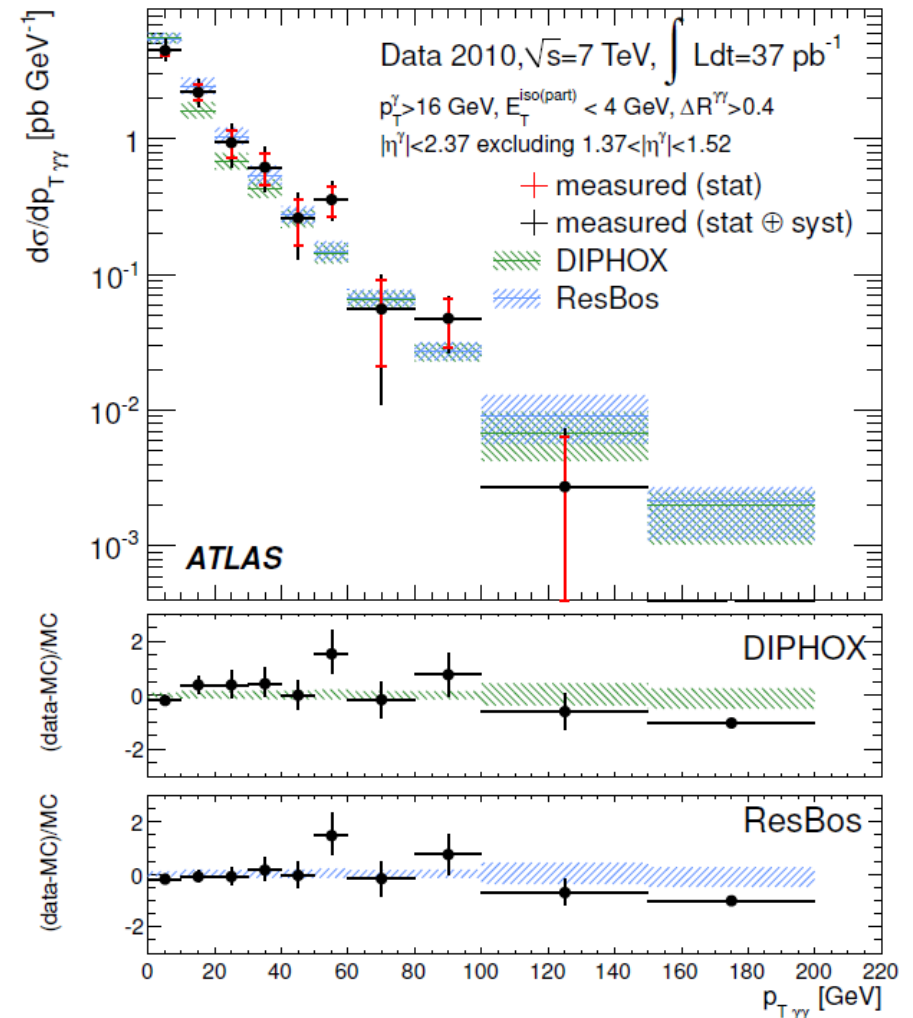
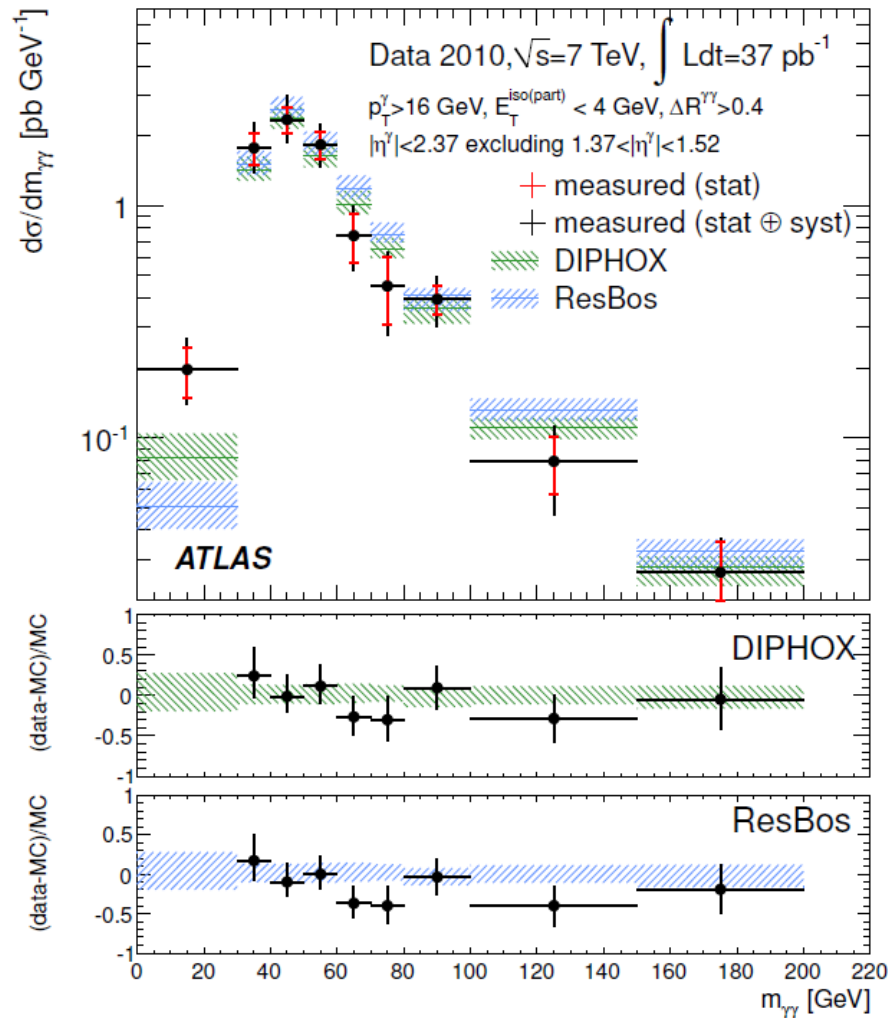
- Require two photons with  $p_T^\gamma > 16$  GeV within acceptance ( $|\eta| < 2.37$ , crack excluded), tight and isolated ( $E_{\text{iso}}^T < 3$  GeV)
- The good news is that all three signal extraction flavours agree fairly well in extracting the signal yield with  $\sim$  comparable systematic uncertainty ( $\sim \pm 15\%$ )



- Electron subtraction with a P/F technique: P is set if the electron is reconstructed only as electron.
- Electron to photon misidentification probability measured on Z data

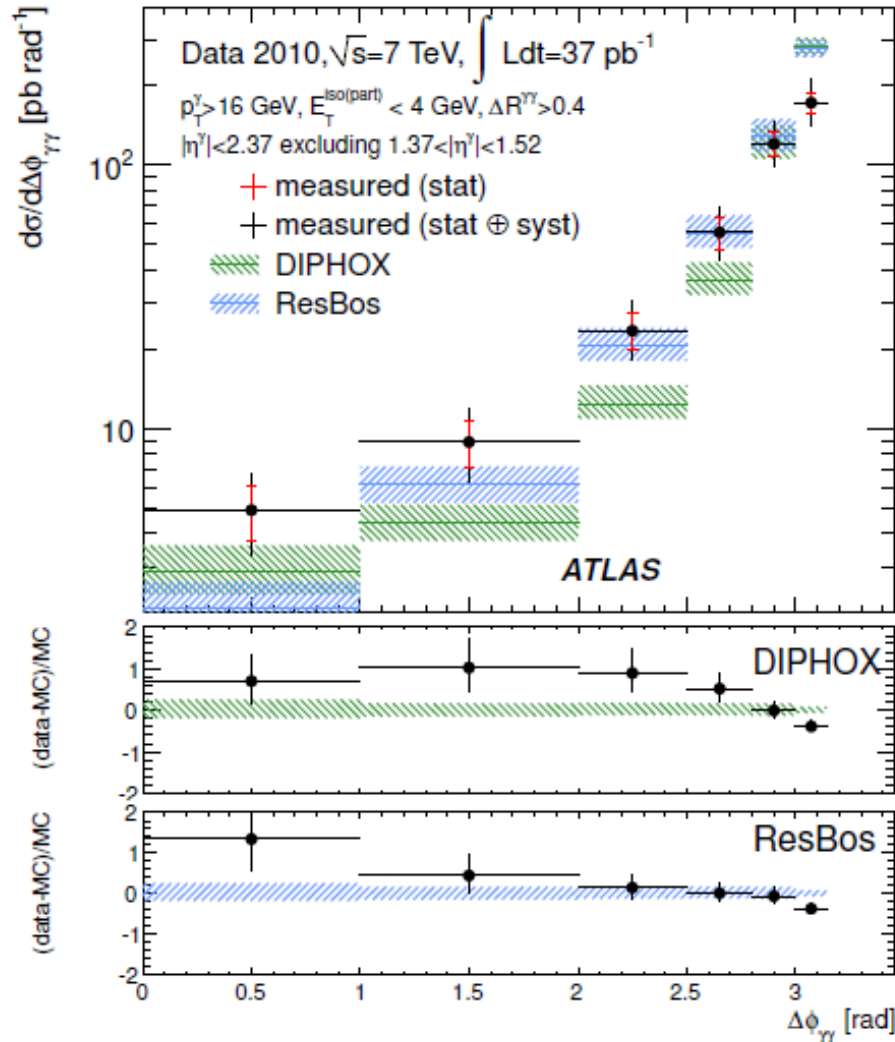


# Di-photon cross sections : data / theory comparison



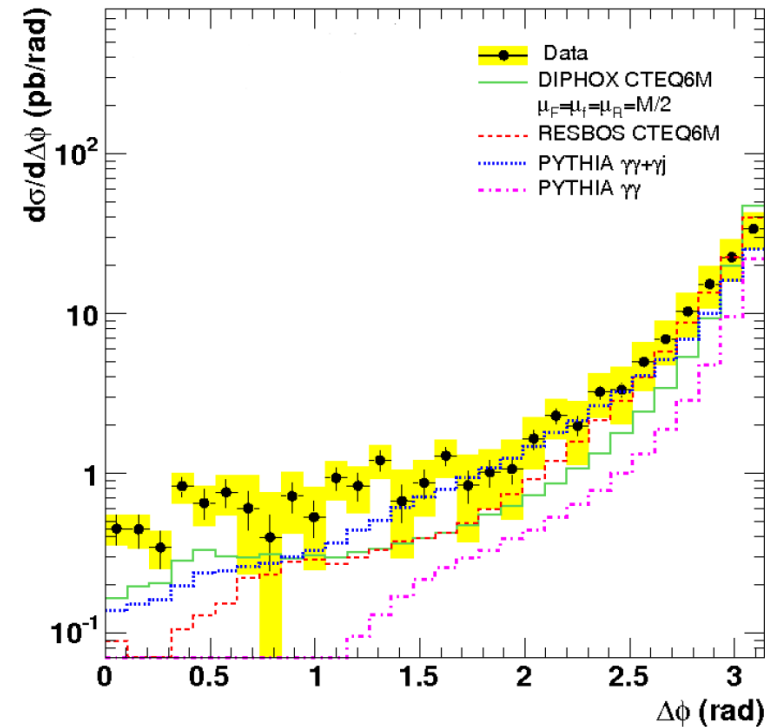
Rather good agreement between data and theory in  $m_{\gamma\gamma}$  (except for low  $m_{\gamma\gamma}$ ) and  $p_{T\gamma\gamma}$

# Di-photon cross sections : data / theory comparison

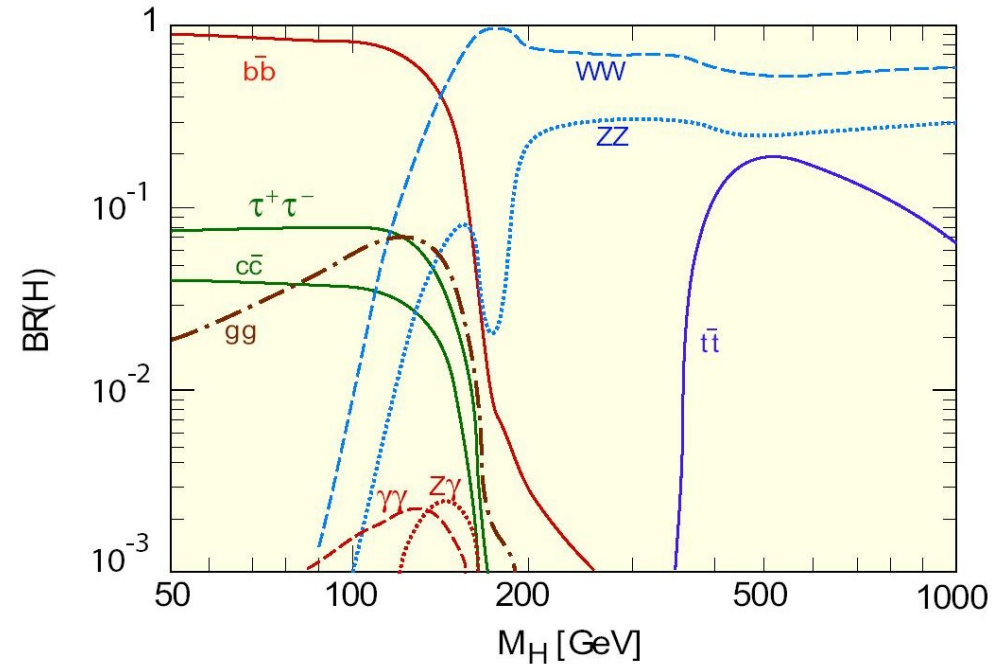


- Some disagreement especially in the low  $\Delta\phi$  region (which is also the low  $m_{\gamma\gamma}$  region) and  $\Delta\phi \sim \pi$
- Qualitatively compatible with the measurements done at the Tevatron (see latest CDF plot below)

arXiv:1106.5123v1



## Search for resonances in the di-photon channel : the Higgs case

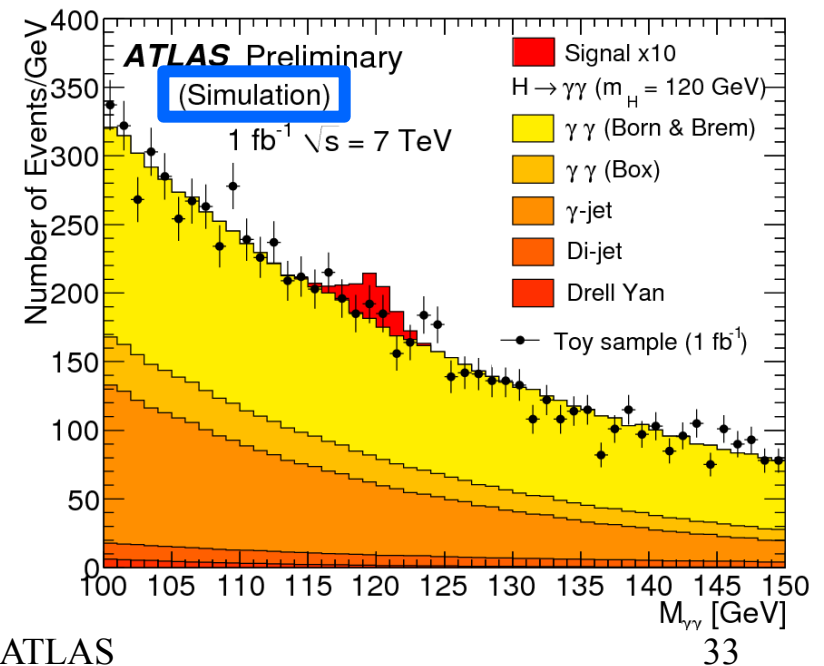


- ❑ The BR of the decay of a SM higgs decay to a photon pair is  $\sim 0.2\%$  (in the 100-160 GeV region)
- ❑ On the other hand it sits in an interesting mass region which is favored by the EW fit

❑ The signal should be visible as a narrow peak on top of an exponential background (irreducible  $\gamma\gamma$ , reducible  $\gamma$ -jet and jet-jet)

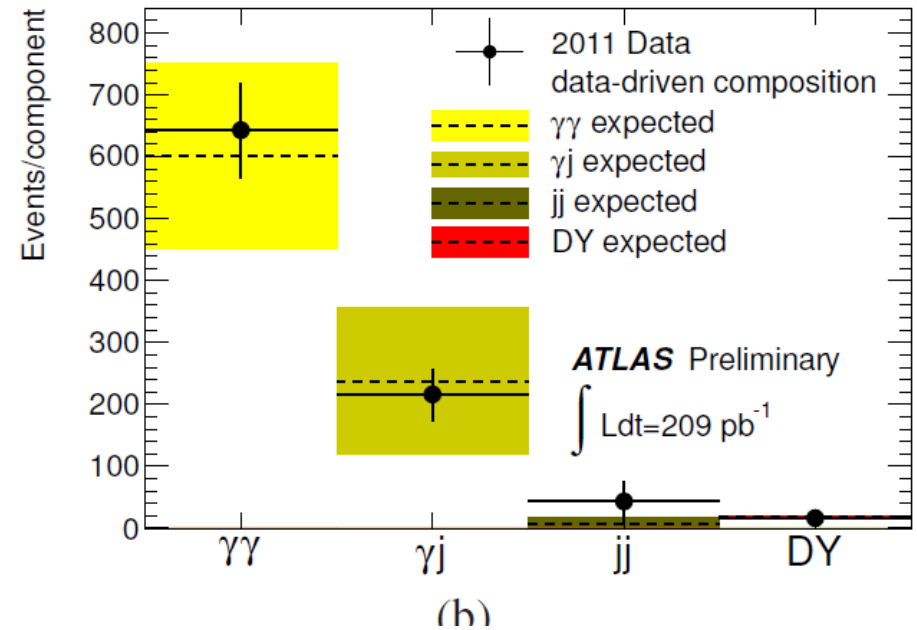
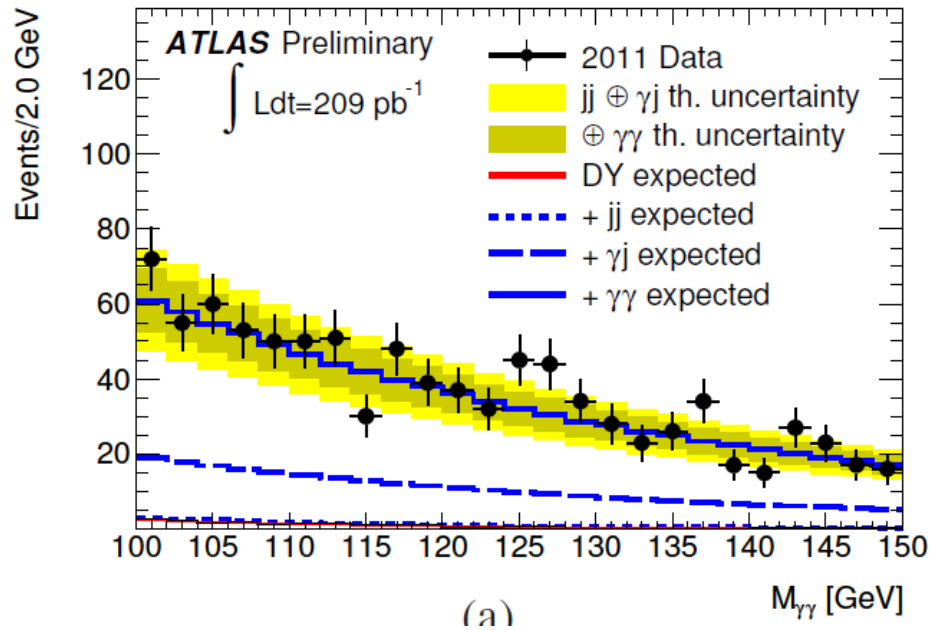
❑ The detector performance and a precise understanding of the details of photon physics is crucial in this analysis

- ❑ calorimeter energy and position resolution
- ❑ jet rejection capabilities



## Di-photon spectrum decomposition

□ 1/5 of the whole available statistic, new results will be available quickly



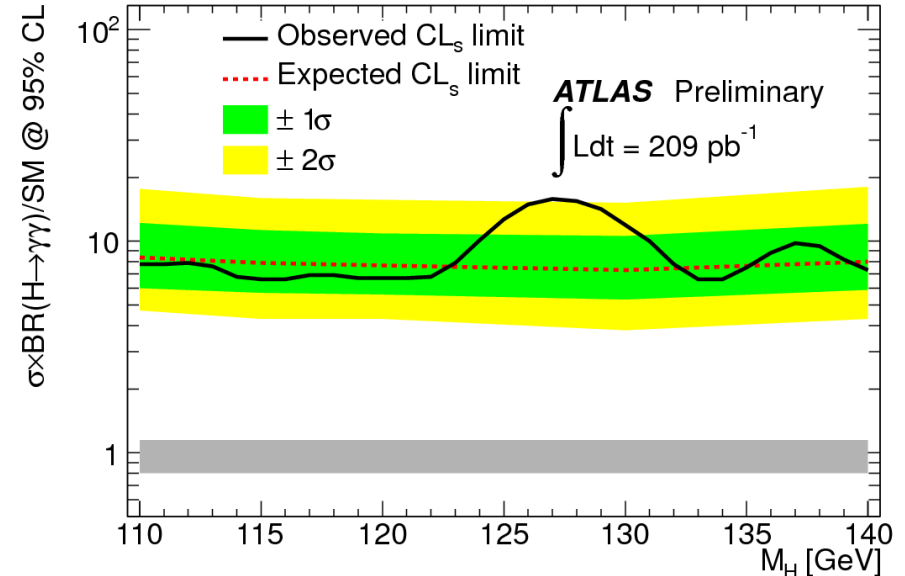
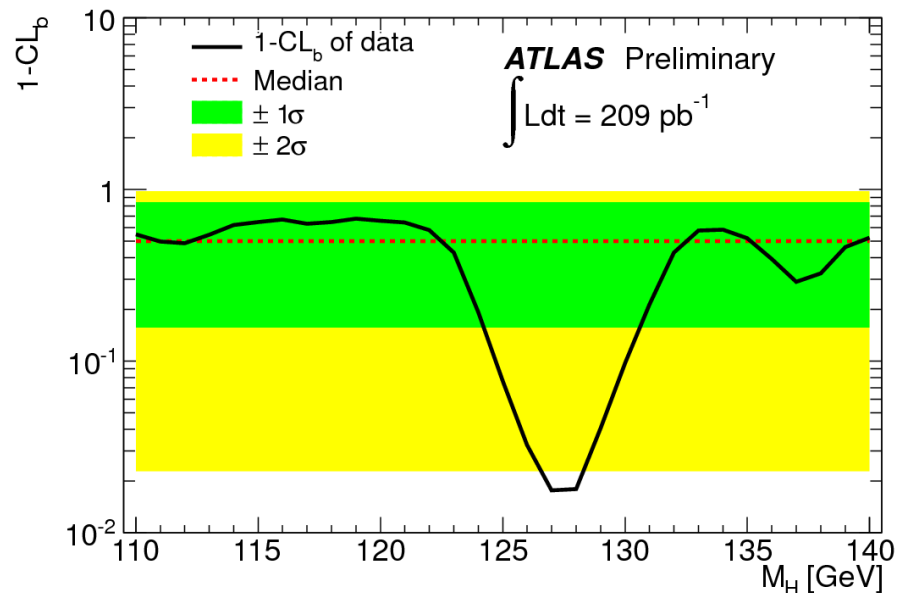
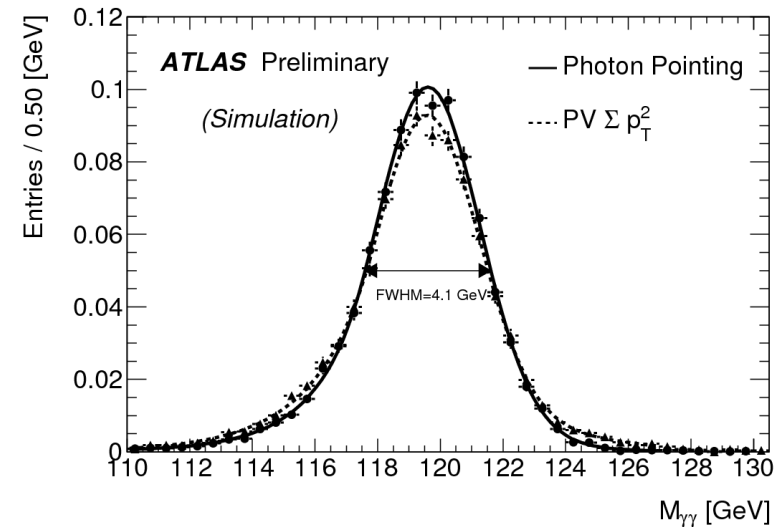
	$N_{\gamma\gamma}$	$N_{DY}$
Expected (MC)	$602 \pm 169$	$18 \pm 2$ (MC stat only)
Measured	$643 \pm 45$ (stat.) $^{+54}_{-71}$ (syst.)	$23.8 \pm 0.6$ (stat.) $\pm 3.8$ (syst.)
	$N_{\gamma j}$	$N_{jj}$
Expected (MC)	$238 \pm 129$	$8 \pm 8$
Measured (Reducible)	$216 \pm 23$ (stat.) $^{+32}_{-54}$ (syst.)	$43 \pm 6$ (stat.) $^{+44}_{-18}$ (syst.)

## Looking for a signal :

❑ A crystal ball + gaussian function is used to model the signal shape ( $\sim 3$  events expected).

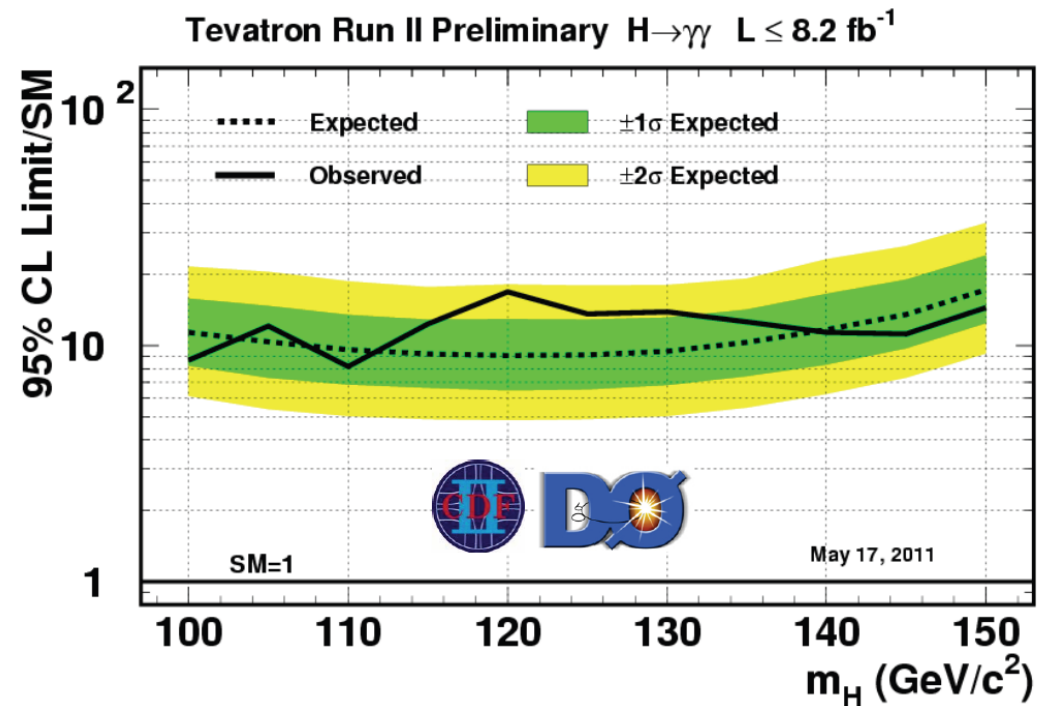
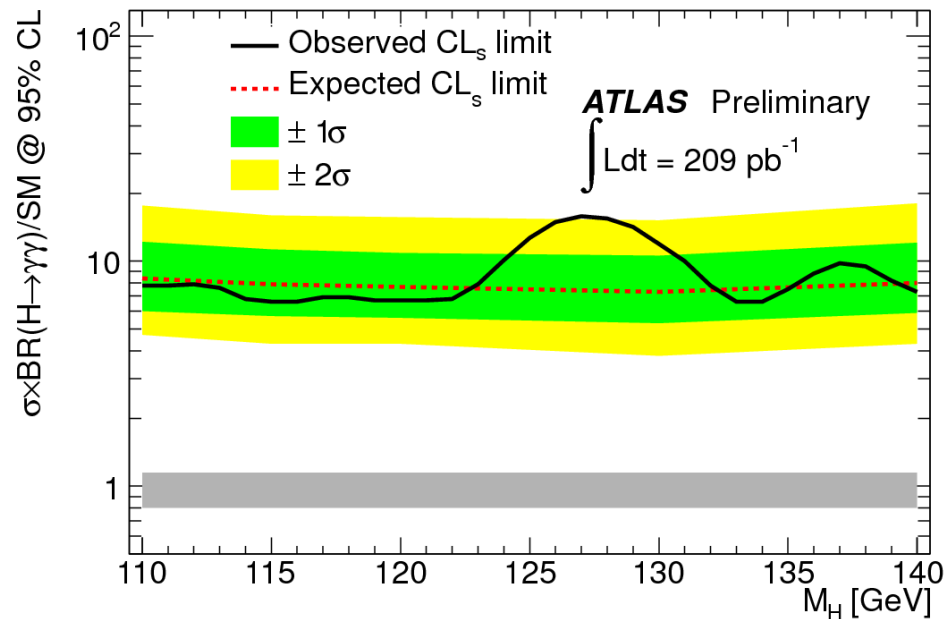
❑ main systematic uncertainties  $\sim 12\%$  on the signal yield and  $13\%$  on the invariant mass resolution (incorporated as nuisance parameters)

❑ Simple exponential to model the background : normalization and shape nuisance parameters



## Comparison with the Tevatron results

- ❑ The expected limit on the Higgs provided by ATLAS alone on the  $H \rightarrow \gamma\gamma$  decay channel is already the most stringent.

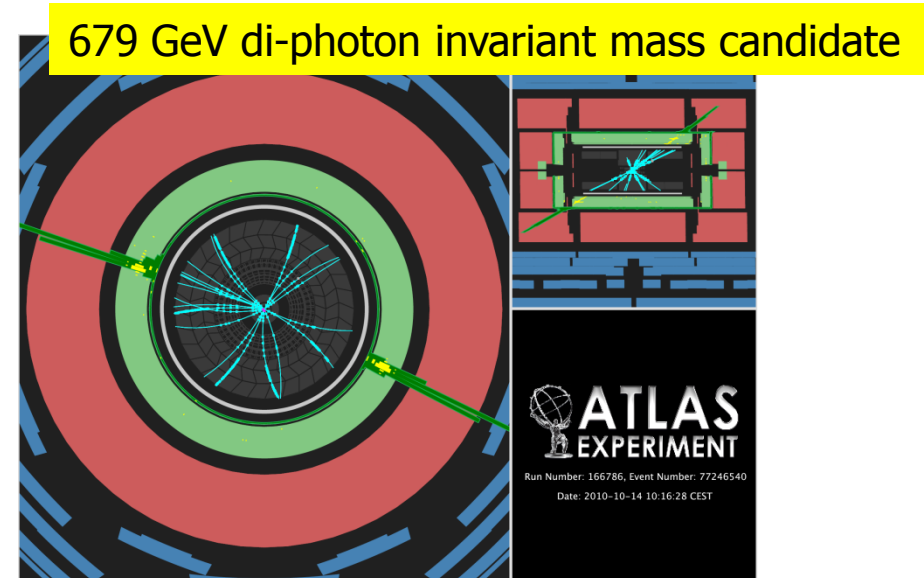


## High di-photon mass resonances

Randall-Sundrum model solves the hierarchy problem by postulating the existence of a fifth spatial dimension that has a warped geometry. In this model SM particles are localized on the 3+1 brane while the gravity is localized on the other

- ❑ The TeV scale is naturally generated from the Planck scale due to a geometric warp factor
- ❑ In the minimal RS model gravitons are the only particles that can propagate in the bulk. Massive graviton excitations are predicted.
- ❑ The lightest KK graviton excitation mass  $m_G$  in the TeV range to cure the fine tuning.
- ❑ The degrees of freedom of the RS model can be expressed in terms of 2 parameters  $m_G$  and  $k/M_{\text{pl}}$  (the coupling to the SM fields)

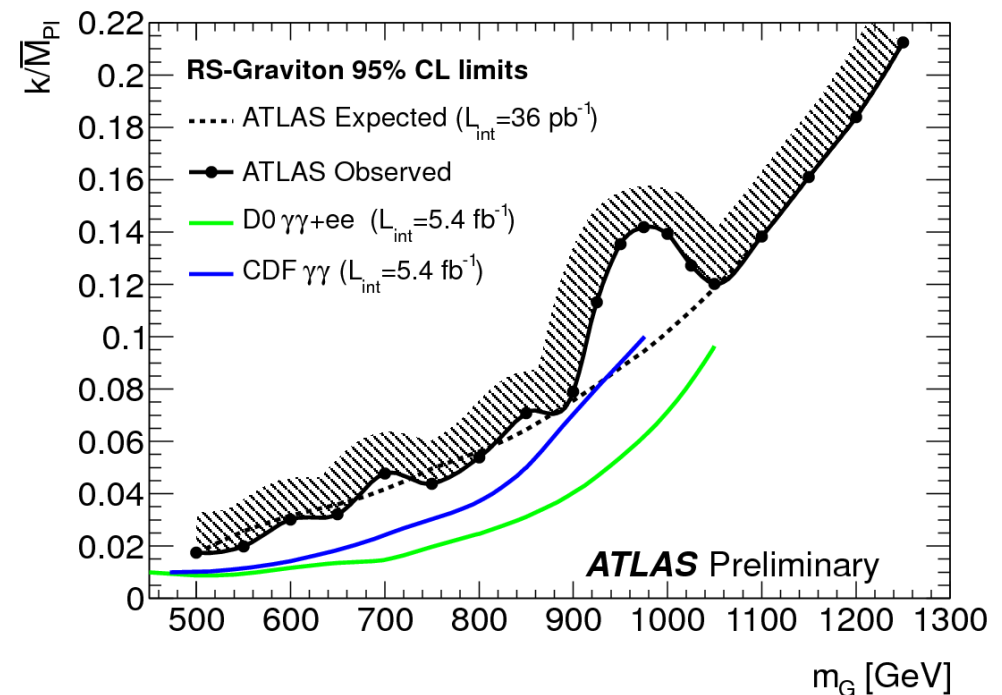
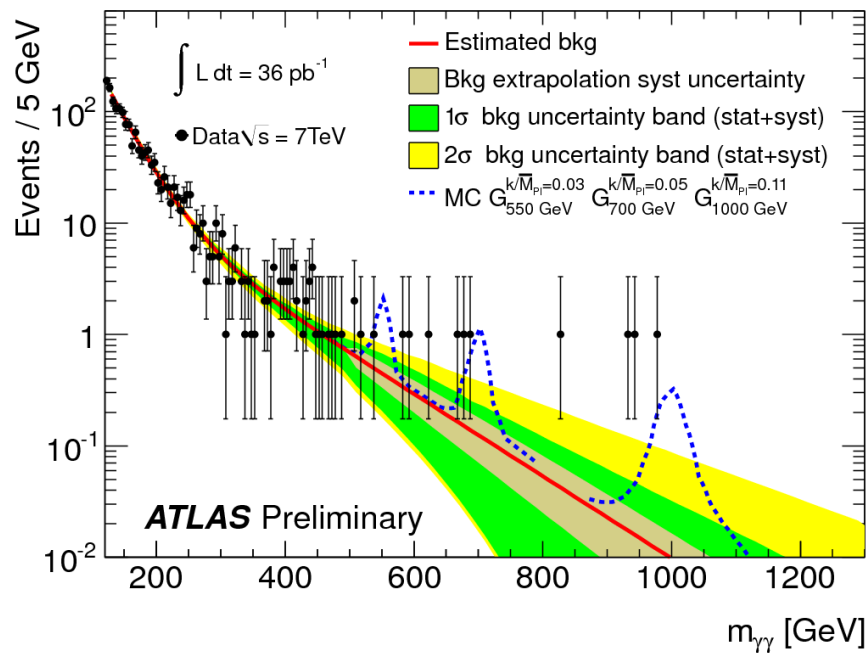
- ❑ Look for events with 2 photon candidates with  $p_T > 25$
- ❑ Only loose selection applied (only cuts on energy in the hadronic calorimeter and shower shapes in the middle sampling of the EM calorimeter)
- ❑ 8090 events in the 2010 data ( $37 \text{ pb}^{-1}$ ) out of which 1650 have an invariant mass  $> 120 \text{ GeV}$



## High di-photon mass resonances

No evidence of a narrow resonance decaying into a pair of photons above the continuum background is observed.

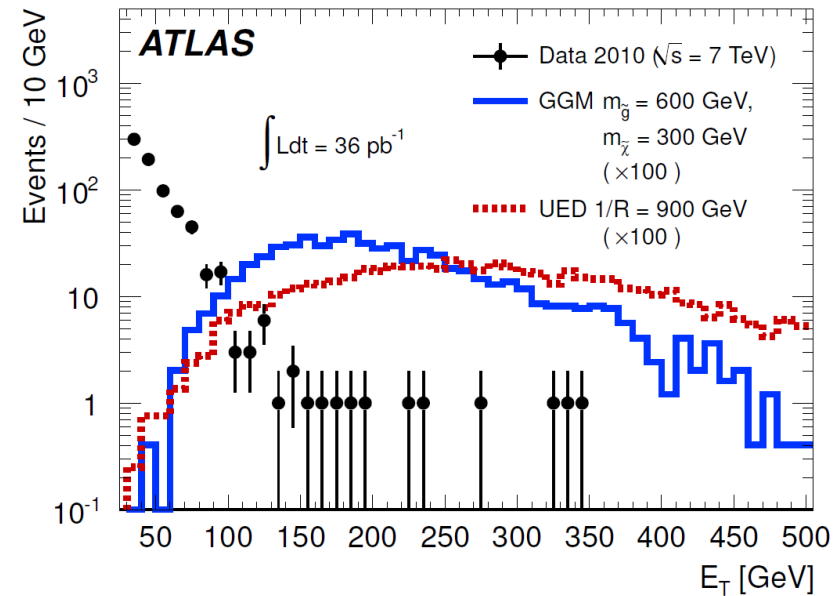
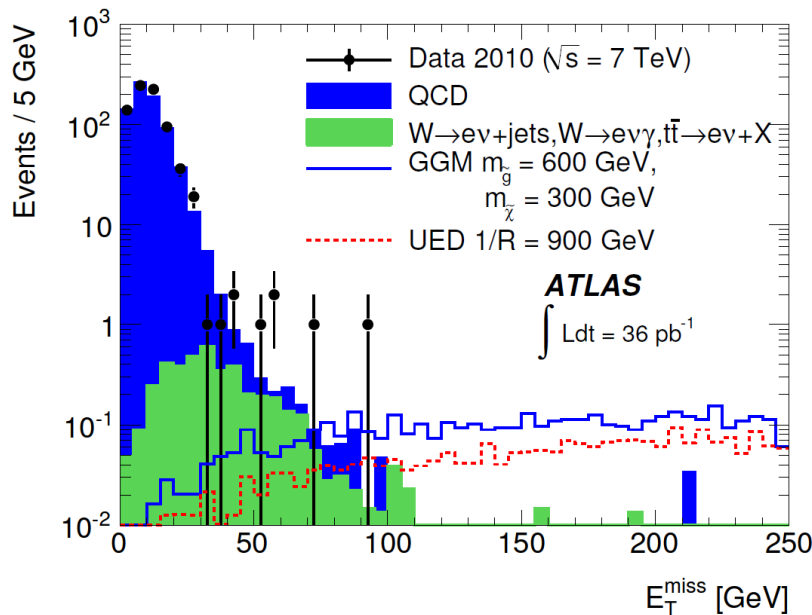
- A. The results exclude at 95% CL a RS graviton of mass below 545 (920) GeV for a coupling of 0.02 (0.1)
- B. The results enlarge the mass range already explored by the Tevatron



## Search for diphoton events and large missing energy

Search for events with 2 photons and large missing energy ( $>125$  GeV) has been performed at ATLAS using  $37 \text{ pb}^{-1}$  of 2010 data. The results are interpreted in the context of GGM-SUSY and UED models predicting an excess wrt to SM expectation

- ❑ No excess is observed in 2010 data (zero events observed)
- ❑ Limits set on production cross sections for new physics models  $< 0.38 - 0.65 \text{ pb}$  for the GGM model and  $< 0.18 - 0.23 \text{ pb}$  for the UED
- ❑ Under the GGM hypothesis, a lower limit on the gluino mass of 560 GeV is determined for bino masses above 50 GeV, while a lower limit of  $1/R > 961 \text{ GeV}$  is set on the UED compactification radius  $R$ . These limits provide the most stringent tests of these models to date.



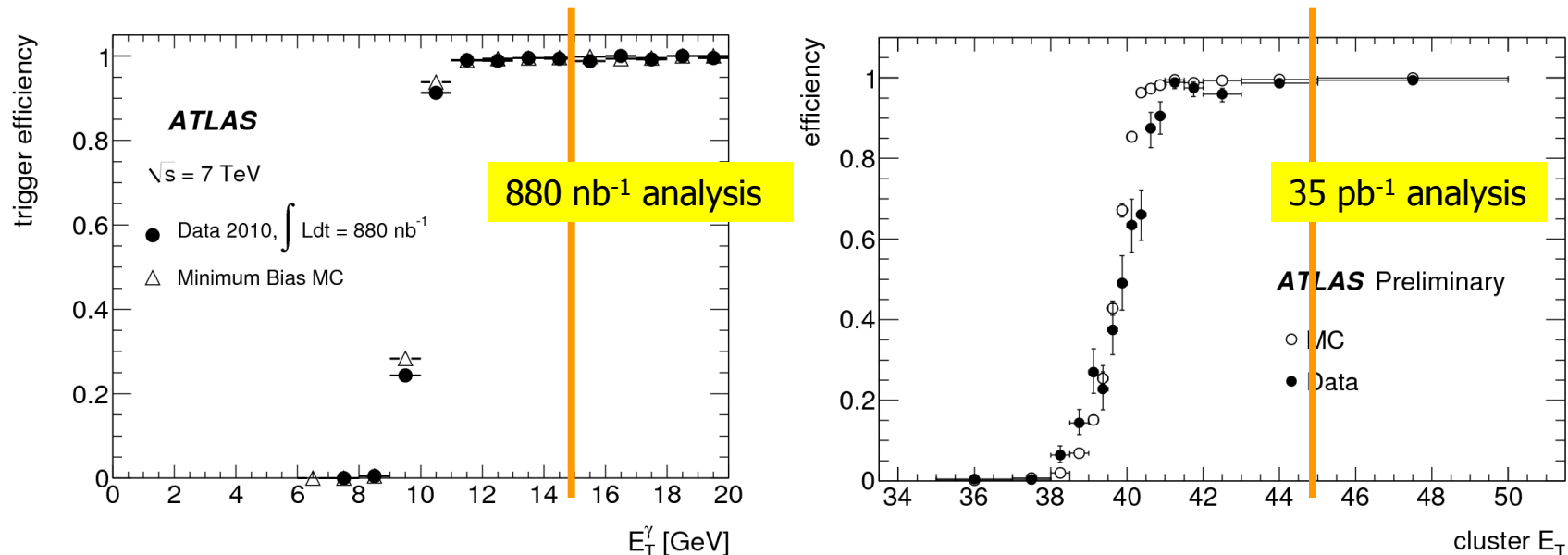
---

## Conclusion :

- A. QCD photons clearly seen and measured in ATLAS :
  - A. first ATLAS inclusive photon cross section published and the new analysis on all 2010 data in under discussion
  - B. Measured di-photon production cross section in 2010 data
- B. Main systematic uncertainties studied and understood. Continuous improvements (and problems) when looking at new data.
  - A. Better understanding of the photon energy scale and resolutions
  - B. Improved photon efficiency studies
  - C. Continuous fine tuning of the isolation calculation (pileup!)
- C. Laid the foundation for solid analyses with photons :
  - A. The SM prompt photon activity will continue in 2011 : photon+(n) jet analysis , photon+heavy flavour, improved inclusive and diphoton analyses, impact of Frixione – style isolation
  - B. Already started addressing seriously the search for a SM Higgs boson decaying into 2 photons. Exclusion limits already better than the Tevatron.
  - C. Exclusion limits for some new physics models involving photons extended

## Reconstruction and trigger efficiency

- ❑  $\epsilon_{\text{reco}}$  (from MC):  $\sim 80\text{-}85\%$  in the barrel ( $|\eta| < 1.37$ ),  $\sim 70\%$  in the endcap ( $1.52 < |\eta| < 2.37$ )
- ❑ significant part of inefficiency (dead readout) recovered in 2011 winter shutdown
- ❑ uncertainties: extra material not in MC (1-2%), generator and fraction of fragmentation photons ( $< 2\%$ ), experimental isolation efficiency (3-4%)



- ❑  $\epsilon_{\text{trig}}$  close to 100% (with  $\sim 1\%$  uncertainty) in the pt range considered in the two different analyses

## Unfolding :

The problem : we are interested in the measurement of the average differential cross section for the production of isolated prompt photons in a certain bin  $i$  of (true)  $E_T$  (integrated over one true  $\eta$  bin  $k$ )

$$\left\langle \frac{d\sigma_i^{\text{isol},k}}{dE_T^{\text{true}}} \right\rangle = \frac{1}{\int \mathcal{L} dt} \frac{N_i^{\gamma, \text{true}, \text{isol}, k}}{\Delta E_{T,i}^{\text{true}}}$$

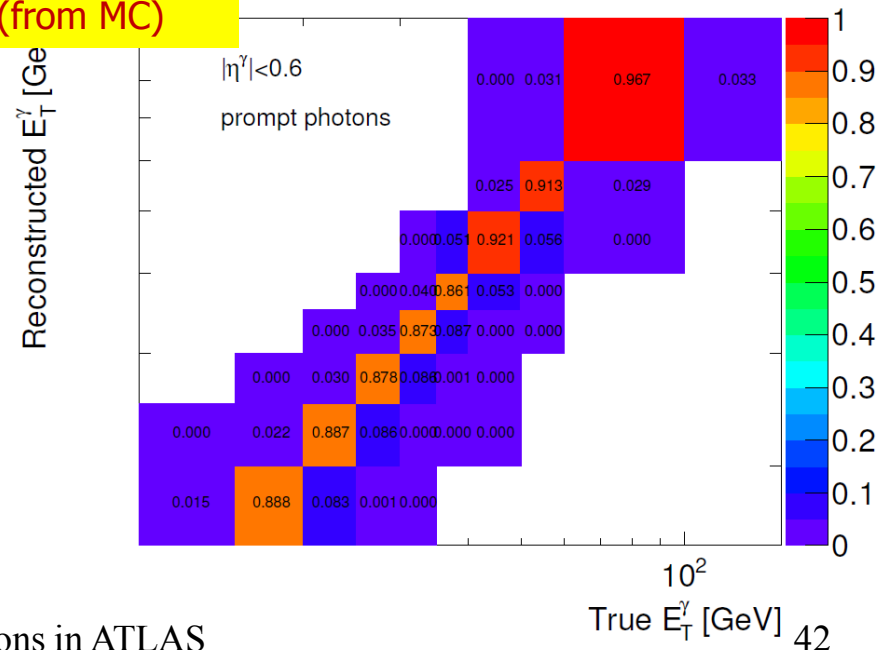
measurement

$$N_i^{\gamma, \text{reco}, \text{isol}, k} = \left( \int \mathcal{L} dt \right) \varepsilon^{\text{trig}} \varepsilon_i^{\text{offl}, k} \sum_j R_{ij}^k \varepsilon_j^{\text{reco}, k} \Delta E_{T,j}^{\text{true}} \left\langle \frac{d\sigma_j^{\text{isol}, k}}{dE_T^{\text{true}}} \right\rangle$$

truth

The elements of  $R_{ij}^k$  represent the probability for a prompt photon of true transverse energy in bin  $j$ , reconstructed in the  $k$ -th  $|\eta|$  bin and having experimental isolation lower than 3 GeV, to have reconstructed transverse energy in bin  $i$ .

Response matrix  
(from MC)



❑ In general not a simple matrix inversion:

- ❑ Bin by bin unfolding: this method works well if the bin-to-bin migrations are small, and transverse energy smearing is smaller than the bin size
- ❑ Bin by bin unfolding agrees within 2% with the full glory procedure
- ❑ Systematic due to energy scale uncertainty (3%) estimated at the unfolding level

## A few more words on isolation

S. Frixione : arXiv:hep-ph/9809397

In the spirit of the cone approach, an alternative definition of the isolated photon has been proposed [27]. After drawing a cone of half-angle  $R_0$  around the photon axis, all the cones of half-angle  $R \leq R_0$  are considered; their definition is identical to the one given in eq. (2), with  $R_0$  replaced by  $R$ . Denoting by  $E_{T,had}(R)$  the total amount of hadronic transverse energy found in each of these cones, the photon is isolated if the following inequality is satisfied:

$$E_{T,had}(R) \leq \epsilon_\gamma p_{T\gamma} \mathcal{Y}(R), \quad (4)$$

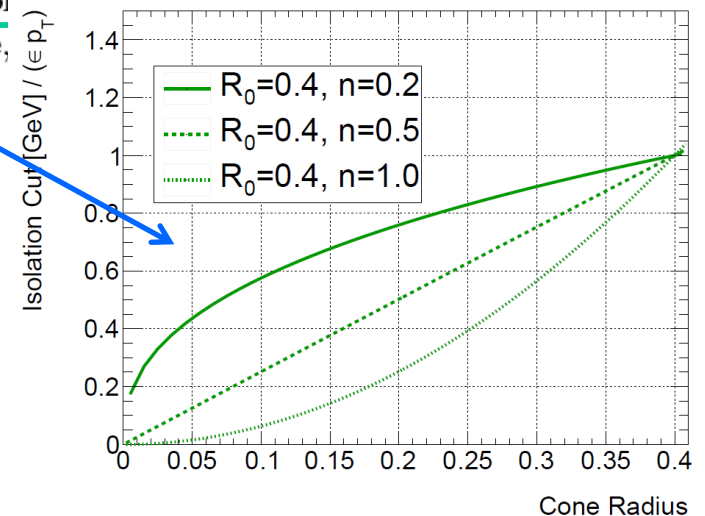
for all  $R \leq R_0$ . A sensible choice for the function  $\mathcal{Y}$  is the following

$$\mathcal{Y}(R) = \left( \frac{1 - \cos R}{1 - \cos R_0} \right)^n, \quad n = 1. \quad (5)$$

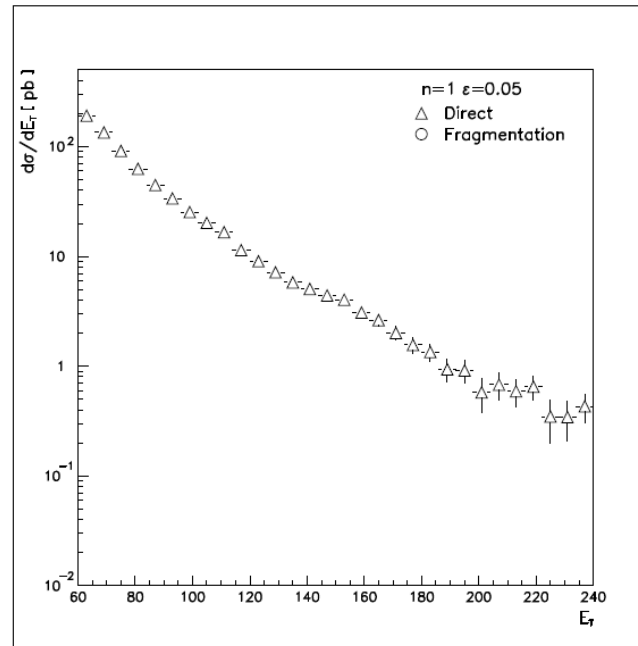
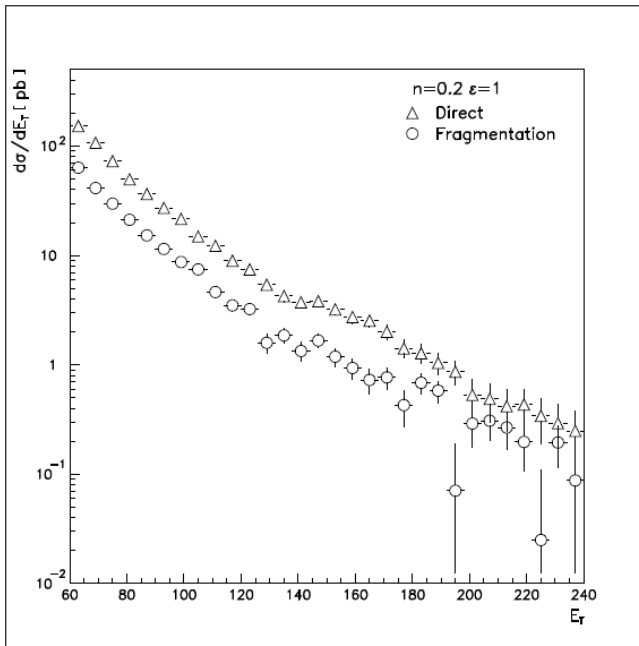
It has been proved in ref. [27] that such a choice allows the definition of an isolated-photon-plus-jet cross section, which is infrared-safe to all orders in QCD perturbation theory. It does not receive any contribution from the fragmentation mechanism. In this case,

❑ This isolation criterium works in theory but not exactly from the experimental point of view:

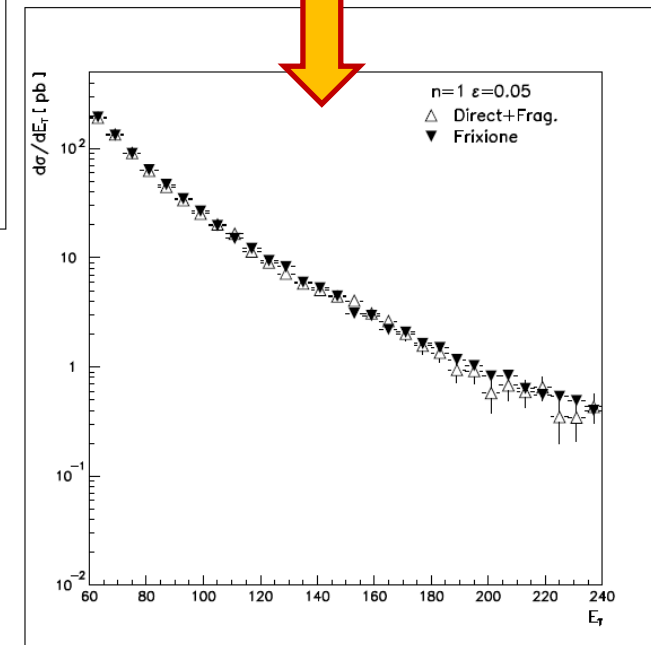
- ❑ the photon has a finite size in our calo and we can't go arbitrarily close
- ❑ the calorimeters have a finite granularity, cones are discrete



## A few more words on isolation

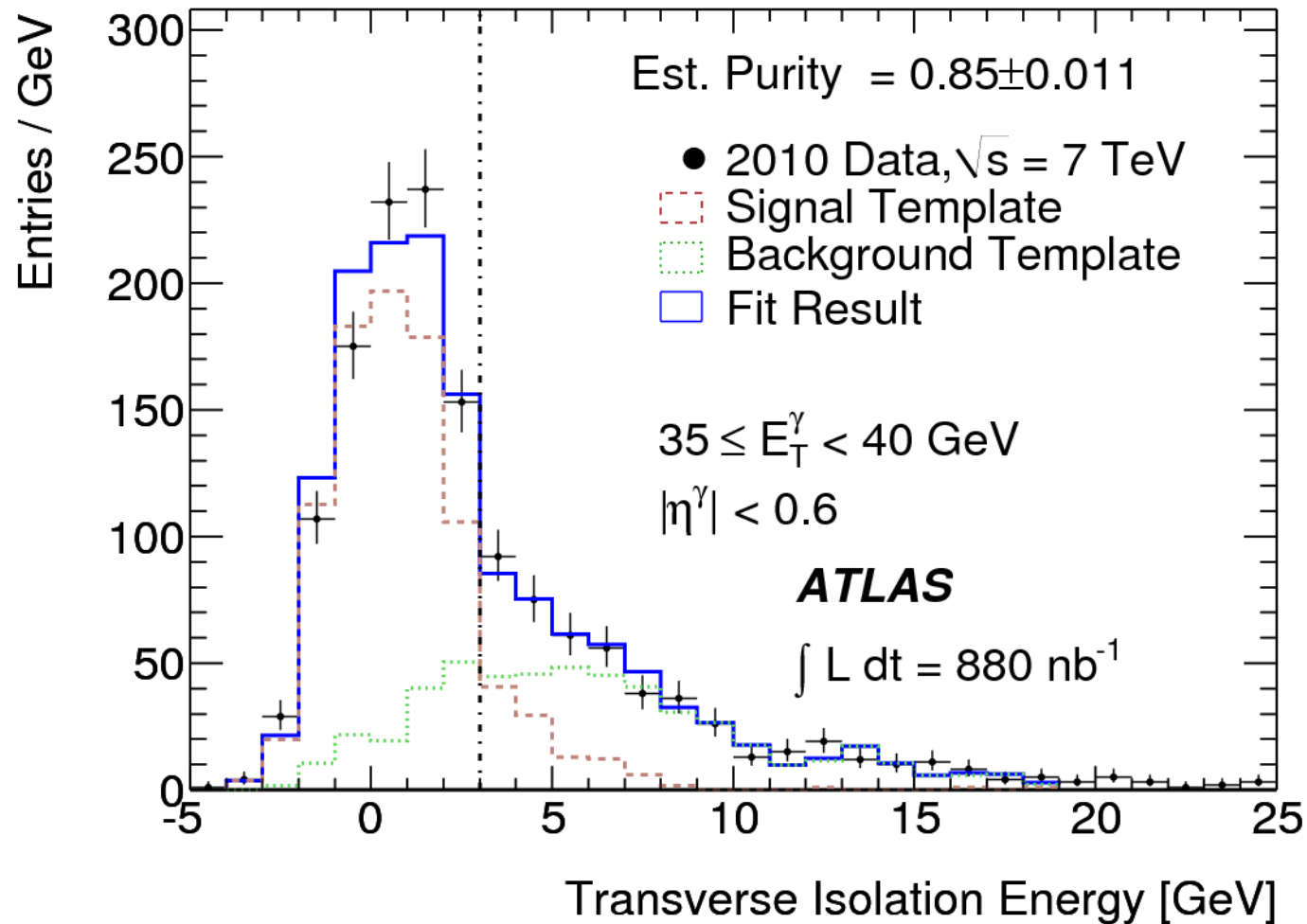


Comparison between discrete (experimental) and continuous (theory) version of Frixione style isolation using JETPHOX



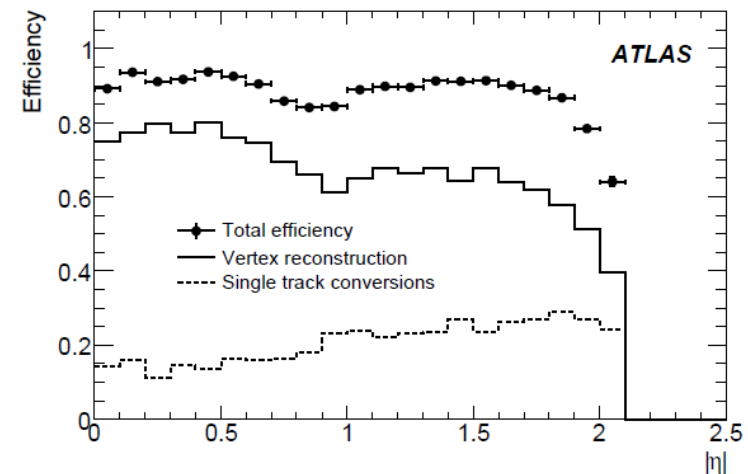
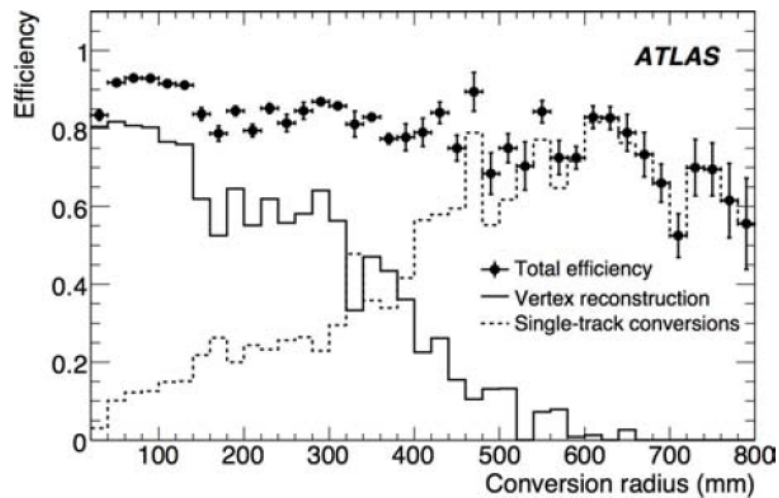
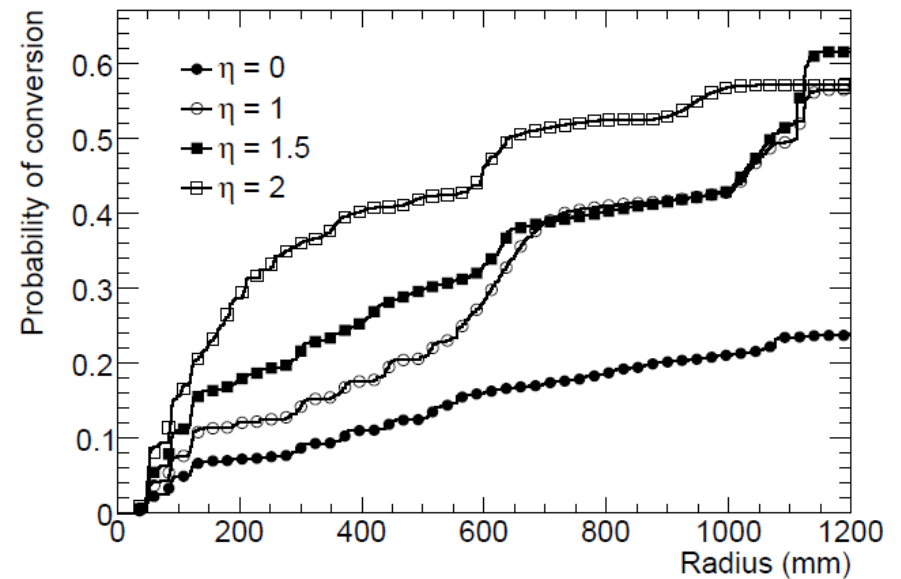
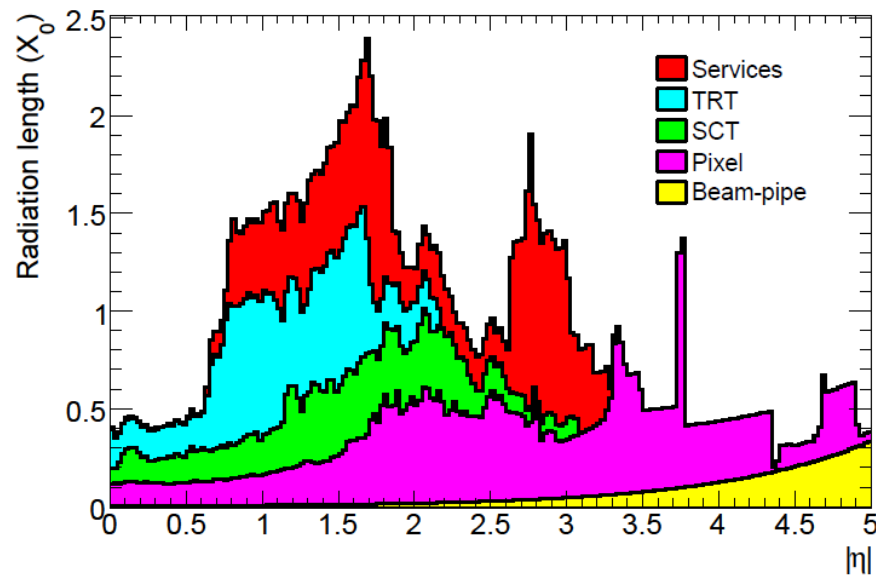
- ❑ With a proper choice of the parameters in the Frixione isolation definition the fragmentation contribution can be considerably damped (at best completely eliminated)
- ❑ A discrete version of the Frixione isolation implemented in JETPHOX : the agreement with the continuous version is fairly good.
- ❑ So yes we have no excuses not to use it to analyze data!

## Signal extraction : isolation template fit



# Conversions

Simulation : arXiv:0901.0512

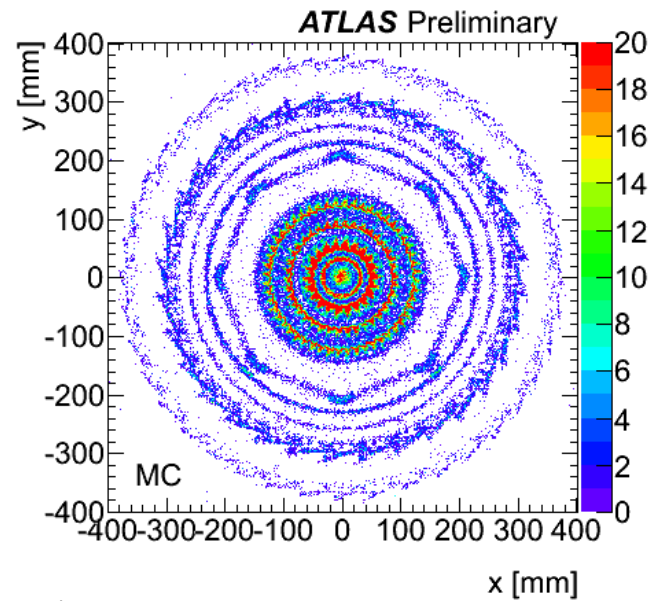
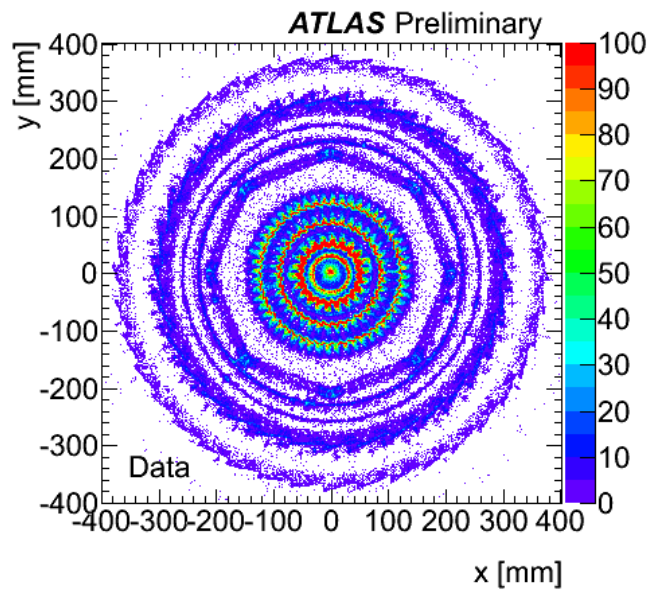
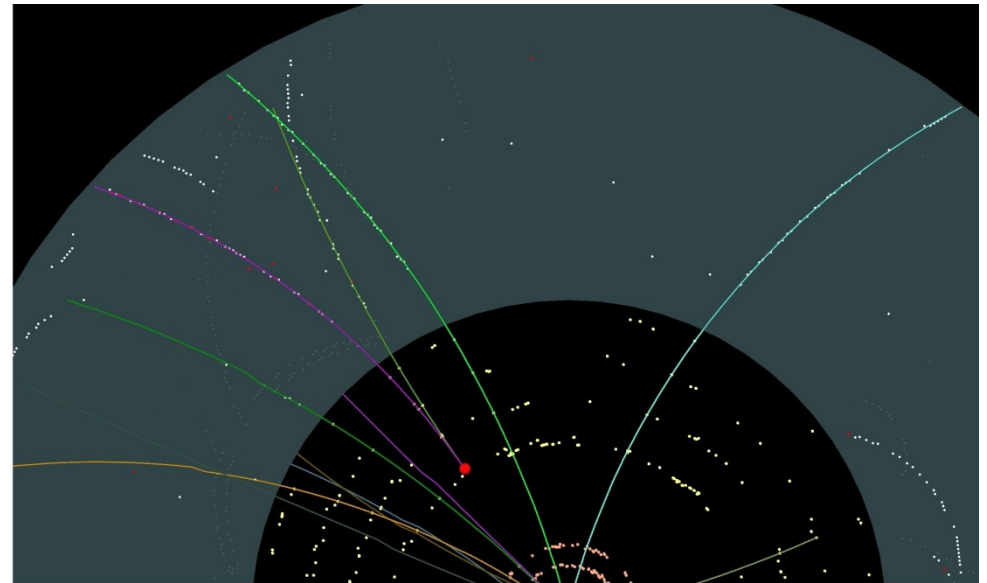
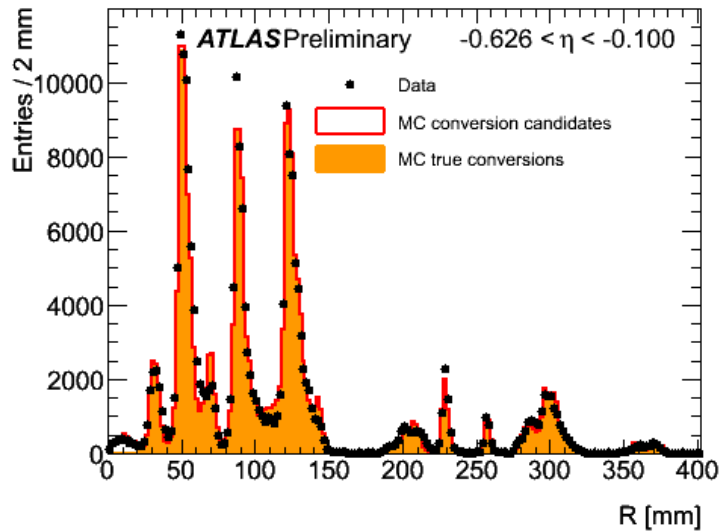


05/07/2011

Physics with photons in ATLAS

46

## Photon conversions



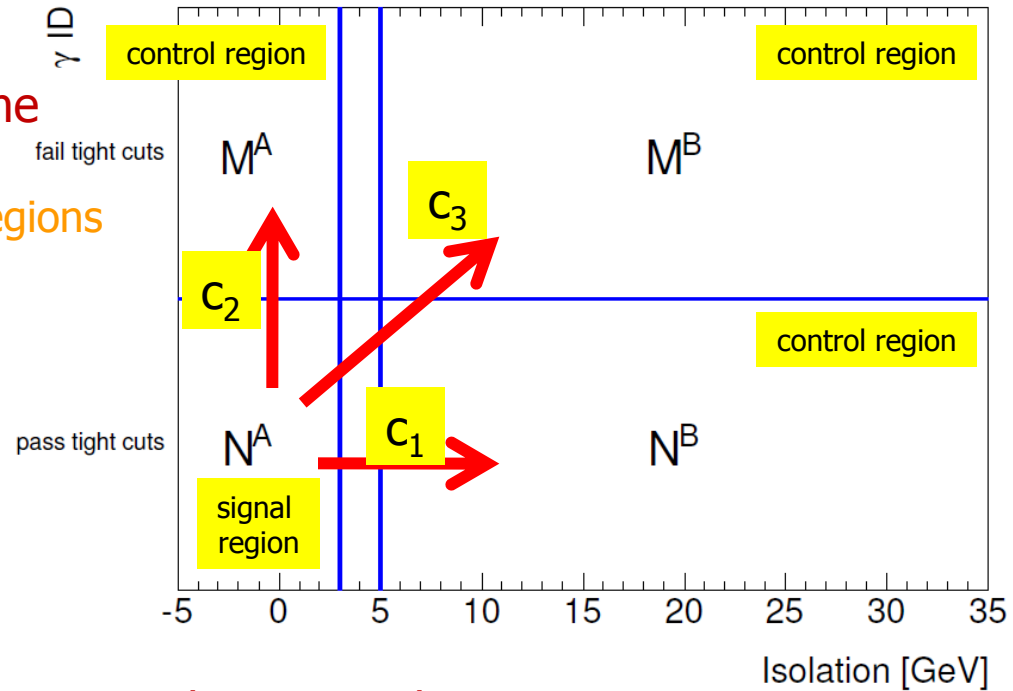
## Background estimation and signal extraction :

If we take correlation and signal leakage in the control regions into account (both from MC)

- $c_x$  : signal leakage in the background control regions
- $R_{mc}$  : background pseudo-correlation factor

$$N_{sig}^A = N^A - \left[ (N^B - c_1 N_{sig}^A) \frac{M^A - c_2 N_{sig}^A}{M^B - c_3 N_{sig}^A} \right] \left( \frac{N_{bkg}^A}{N_{bkg}^B} \frac{M_{bkg}^B}{M_{bkg}^A} \right)$$

(The term  $R_{mc}$  is circled in blue in the original image, representing the ratio of background yields in the two channels.)



Signal leakage coefficients are evaluated from MC and varies with  $P_T^\gamma$

- $C_1$  is  $\sim 3\%$  at low  $P_T$  growing to  $\sim 10\%$  at high  $P_T$  mainly due to 'fragmentation' photon which are accompanied by some hadronic activity
- $C_2$  is  $\sim \text{few } \%$  decreasing rapidly with  $P_T$
- $C_3$  is  $\sim \text{negligible}$  in all  $P_T$  and  $\eta$  bins
- Systematics on  $C_x$  coefficients assessed using PYTHIA and HERWIG fully simulated samples, and separating into pure direct (from hard interaction) and 'brem' contributions (from QED radiation)
- $R_{mc}$  : background pseudo-correlation factor taken from dijet like MC  $\sim 1$

## Back to photon isolation

❑ As for the inclusive analysis the photon isolation plays a crucial role in the diphoton analysis as well.

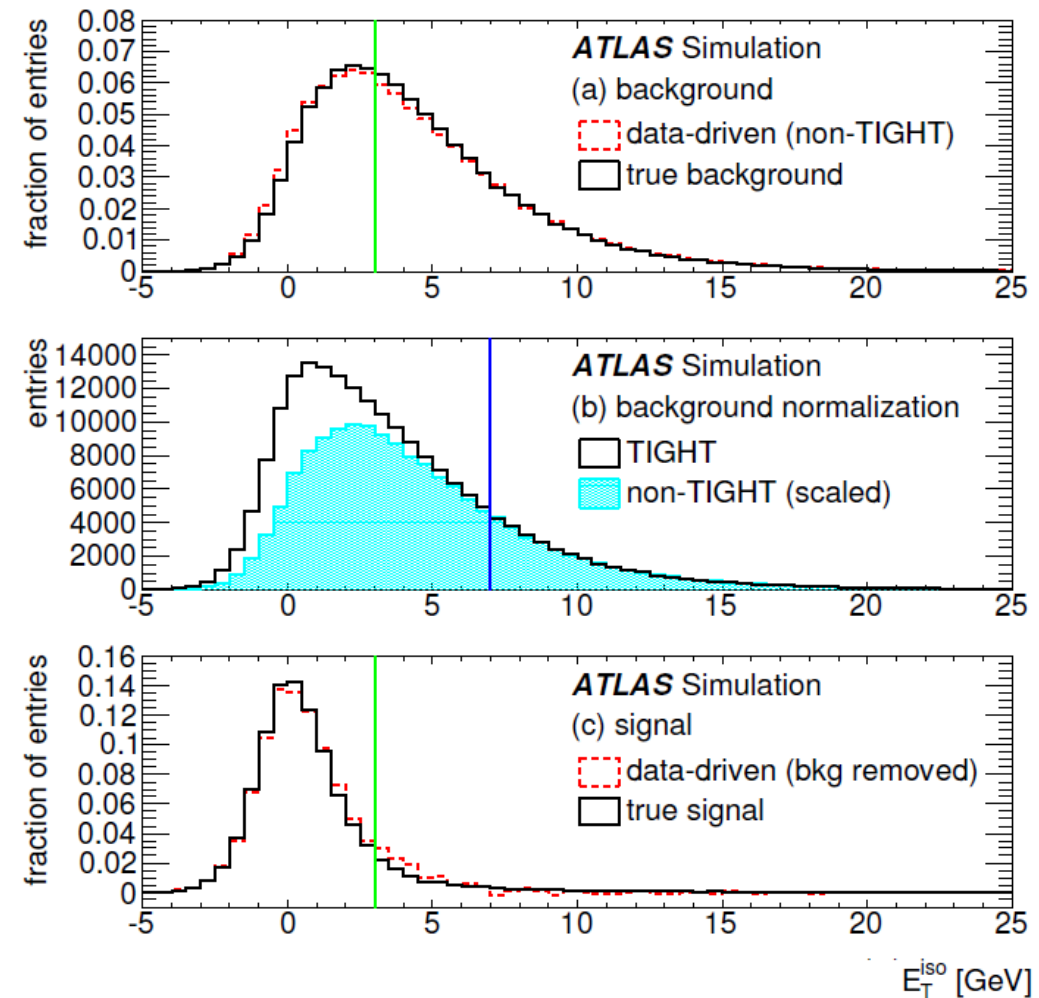
❑ The key point is the possibility to extract isolation energy profiles for signal and background directly from data using the same 2D-sidebands classification

❑ Plot on the right is a nice consistency test on dijet-like PYTHIA MC events.

❑ fig (a) : non tight candidate isolation energy profile matches the one of the true background

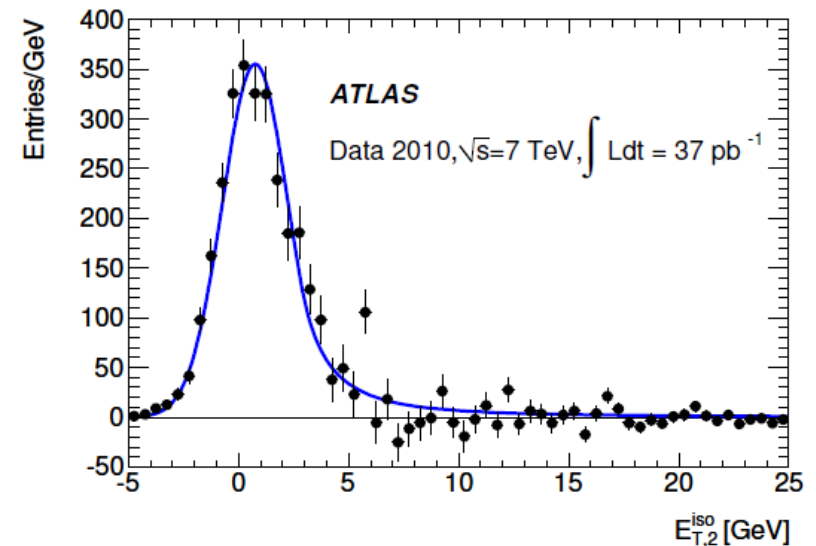
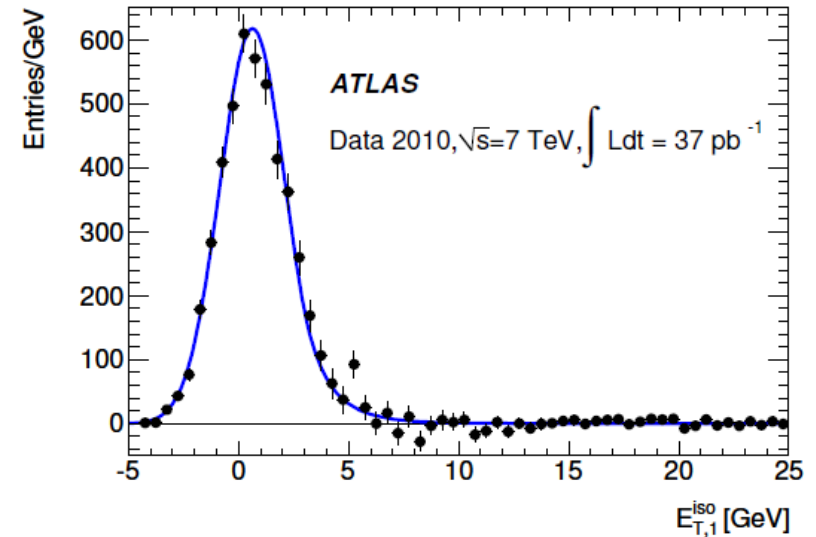
❑ fig (b) : no signal for  $E_T^{\text{iso}} > 7$  GeV so the non-tight can be normalized to the tight in this area

❑ fig (c) by difference the signal profile can be extracted



## Photon isolation energy again...

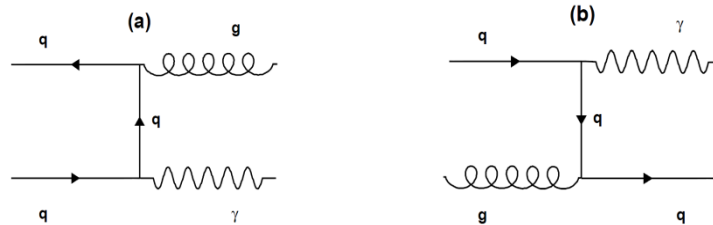
- ❑ Or you can extract the isolation profiles from a clean electron sample from W and Z
- ❑ Electrons and photons are different :
  - ❑ electrons suffer from bremsstrahlung in the material in front of the calo affecting the core of the distribution
  - ❑ fragmentation photons contribute to the tails of the photon isolation distribution
- ❑ Correcting the differences using MC return isolation profiles consistent with the ones extracted from the 2D sideband method



## Prompt photon production:

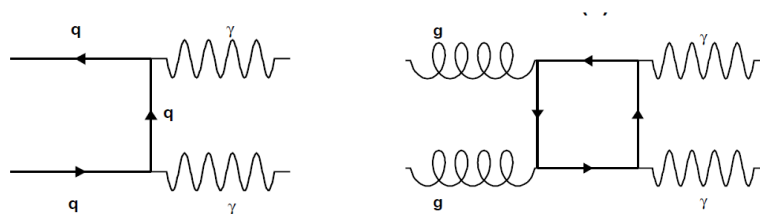
Look to events with one or two photons in the final state : mainly from purely QCD/QED diagrams like the following

- Single prompt photon production (LO), Direct process : true (almost) isolated photon!



sensitive to gluon density inside the colliding proton already at LO. Direct probe of the strong process: no complications due to jet related uncertainties

- Double prompt photon production



Main background to H to gamma gamma decay search